12-2022

Water Hardness Removal by Electrochemical Precipitation in a Continuous Flow Condition Using Conductive Concrete as Cathode

Tahsin Tareque
The University of Texas Rio Grande Valley

WATER HARDNESS REMOVAL BY ELECTROCHEMICAL PRECIPITATION IN A CONTINUOUS FLOW CONDITION USING CONDUCTIVE CONCRETE AS CATHODE

A Thesis

by

TAHSIN TAREQUE

Submitted in Partial Fulfillment of the
Requirements for the Degree of
MASTER OF SCIENCE

Major Subject: Civil Engineering

The University of Texas Rio Grande Valley

December 2022

WATER HARDNESS REMOVAL BY ELECTROCHEMICAL PRECIPITATION IN A CONTINUOUS FLOW CONDITION USING CONDUCTIVE CONCRETE AS CATHODE

A Thesis

by

TAHSIN TAREQUE

COMMITTEE MEMBERS

Dr. Jong Min Kim

Chair of Committee

Dr. Philip Park

Committee Member

Dr. Thang Pham

Committee Member

December 2022

ABSTRACT

Tareque, Tahsin, Water hardness removal by Electrochemical precipitation in a continuous flow condition using conductive concrete as cathode. Master of Science (MS), December, 2022, 59 pages, 29 figures, 9 tables, references, 97 titles.

This study focuses on the electrochemical precipitation (EP) process to reduce excess water hardness from the Lower Rio Grande Valley (LRGV) tap water using electrically conductive concrete as cathode in a continuous flow condition. LRGV tap water is extremely hard with hardness more than 350 mg/L as $CaCO_3$. Humans can pleasantly consume water with hardness less than 150 mg/l as $CaCO_3$ according to World Health Organization (WHO). Hard water is also known to cause mechanical problems to boilers and heat exchangers. In this process, electricity is passed through electrodes submerged in electrolyte, which causes an alkaline environment around the cathode and precipitate water hardness. Conventional studies on electrochemical hardness removal have used sacrificial metal cathodes which makes the treatment very expensive and unsustainable. However, electrically conductive concrete cathode in this study is made with conductive graphite flakes thus making the system more durable and sustainable. In this study, data will be collected with changes in Current density, flow rate/hydraulic retention time, the total reaction time to analyze their impact on water hardness concentration in tap water. Preliminary research findings showed that an increase in applied current density, reaction time, and a decrease in flow rate achieved greater water hardness removal. If successfully developed, proposed technology will enable municipalities and industries to significantly reduce water hardness on site.

DEDICATION

Thanks to the almighty. My Journey at UTRGV for the master's studies would not have been possible without the love and support of my family and friends. I dedicate this work to my mother Shajeda Begum and Father Md Tarek Chowdhury. It all started from their struggle and sacrifices. All credit goes to them that I enjoy living every single day of my life.

ACKNOWLEDGMENTS

I would acknowledge my supervisor Dr. Jong min Kim. He was not only an excellent academic supervisor, but also turned me into the person I am today. Thanks to him I was able to conduct this research with confidence and pride. Also, I would like to mention Dr. Philip Park who had been meticulously guiding us through thick and thin.

TABLE OF CONTENTS

Page

LIST OF TABLES

Page

LIST OF FIGURES

Page

CHAPTER I

INTRODUCTION

Water is an essential commodity for humans for drinking, domestic and industrial uses. The ever-growing human population and continuous industrialization have increased the demand for potable and clean water. (Chen *et al.* 2004)

Among many impurities in water, hardness is a minor water quality parameter that is not regulated by US Environmental Protection Agency (USEPA). However, excess water hardness should be reduced to moderate level or below to prevent aesthetical problems like staining in residents and mechanical problems like pipe clogging in industries (Gabrielli *et al.*, 2006; Hasson *et al.*, 2010). According to Water Quality Association, water with hardness of 180 mg/L as $CaCO_3$ or greater is very hard water while moderately hard water contains hardness concentration of 60 – 120 mg/L as $CaCO_3$.

Hardness enters groundwater as the rainwater or surface water infiltrates through minerals containing calcium or magnesium. The most common sources of hardness are limestone and dolomite. Hard water is usually defined as water, which contains a high concentration of calcium and magnesium ions (Yildiz *et al.* 2003; Kabay *et al.* 2002). Also, hardness can be caused by several other dissolved metals; those form divalent or multivalent cations, including aluminum barium, strontium, iron, zinc, and manganese. Normally, monovalent ions such as sodium and potassium do not cause hardness. These divalent cations tend to bind with anions in the water

and form stable salts. The type of anion found in these salts distinguishes between the two types of hardness-carbonates and non-carbonate hardness.

Carbonate hardness is caused by the metals combined with a form of alkalinity. Alkalinity is the capacity of water to neutralize acids and is attributed to compounds such as carbonate, bicarbonate, hydroxide, and sometimes borate, silicate, and phosphate. In contrast, non-carbonate hardness forms when metals combine with anything other than alkalinity. Carbonate hardness is sometimes called temporary hardness because it can be removed by boiling water. Non-carbonate hardness cannot be broken down by boiling the water, so it is also known as permanent hardness. Total hardness is the summation of both temporary and permanent hardness caused by calcium and magnesium salts.

Water hardness can be divided into soft (0-75 mg/L of CaCO3), moderate (between 75 and 150 mg/L), hard (between 150 and 300 mg/L), and very hard (more than 300 mg/L of CaCO3) (Kalash et al., 2015b). It is well known that people like to drink water with a hardness of no more than 300 mg/l as CaCO3 (Organization, 2010). Water hardness should be maintained between 80 and 100 mg/l as CaCO3, according to American Water Works Association (Kalash et al., 2015b). Untreated groundwater has a lot more hardness than what Kalash et al. and WHO (2010) recommend (2015). In the USA alone, 44% of the population, including 99% of the rural population depends on groundwater as a primary source of drinking water, which accounts for 20% of total water withdrawals nationwide (USGS, 2005; NGWA, 2010). A large percentage of united states population is prone to hard water (Fig 1).

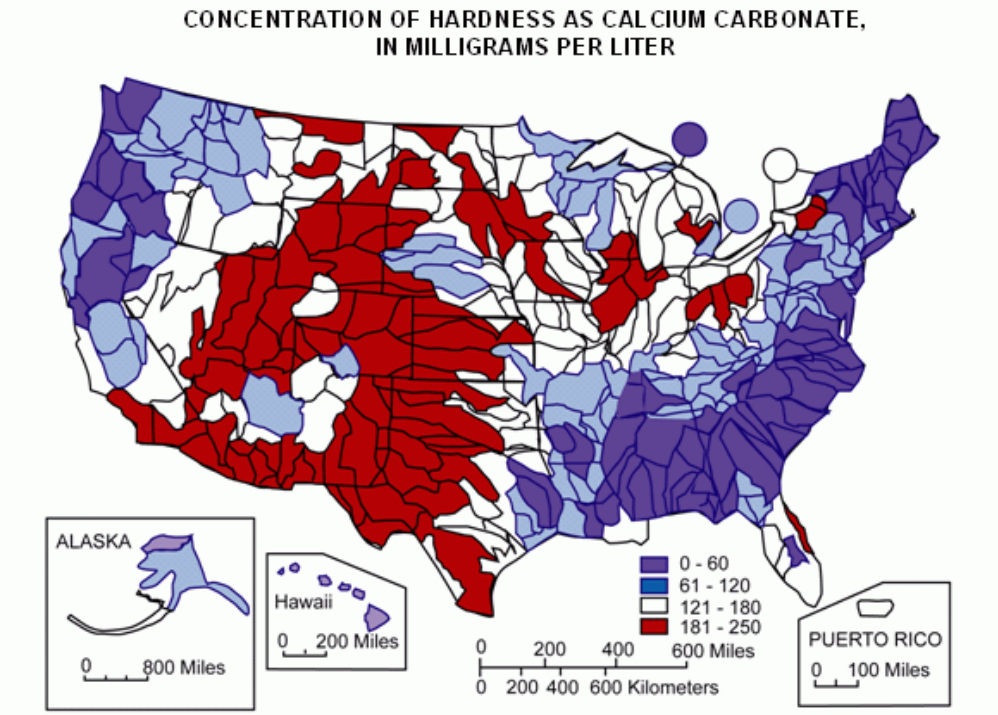

Figure 1: Hardness Concentration map of United States (USGS)

The mechanical problems associated with very hard water involve development of excess scales in pipes, which leads to clogging water pipes, coating heat elements in boilers and cooling towers to reduce heat transfer efficiencies (Lima *et al.* 2004; Park *et al.* 2007; Sanjuan *et al.* 2019). Scaling from water hardness also impairs filtration efficiency of membranes. These problems associated with hard water results in the replacement of the damaged parts and increase in the energy loss and cost associated with it. It is very important to remove excess water hardness in process water and prevent scaling for industries.

There are two major technologies have been adopted to remove water hardness, chemical and physical based. Chemical based technologies include chemical precipitation and ion exchange,

which have been used the most extensively to date (Gabrielli *et al.* 2006; Luan *et al.* 2019; Yu *et al.* 2018). The other group of treatment methods are reverse osmosis, electrodialysis, nanofiltration, crystallization, distillation, and evaporation (Low *et al.* 2008; Verissimo *et al.* 2006; Bequet *et al.* 2000; Tabatabai *et al.* 1995). These physical hardness removal technologies require large energy thus they are very expensive. Chemical treatments produce byproducts that are difficult to dispose of and adds to the total cost of treatment. There are other novel treatment technologies that may overcome the disadvantages of the existing water softening technologies. Electrochemical technology is one of them.

Electrochemical technology has been widely used for water treatment without any chemical additives. It is relatively simple to install and operate, environment-friendly, and versatile. (X. Hao *et al.*, 2019). Research subgroups of electrochemical water treatment technology include electroflocculation, electrochemical disinfection (G. Wuqi *et al.*, 2015), microbial fuel cell technology (Y. Wang *et al.*, 2020), electrochemical scale removal technology (Y. Yu *et al.*, 2018), etc. Among them, electrochemical scale removal technology can be used to remove scale forming water hardness by electrochemical precipitation (EP) and electrocoagulation (EC) (E. Helmy *et al.*, 2017; M. Malakootian *et al.*, 2010). In addition to scale removal capability, the anode produces oxidants in the reactor, which kill microorganisms and algae (X. Zhang *et al.*, 2020; J. Li *et al.*, 2019; D. Shao *et al.*, 2020).

Previous electrochemical treatment experiments (Gabrielli et al., 2006; Hasson et al., 2008; Lédion and Leroy, 1994; Sanjuán et al., 2019a) revealed sustainable hardness removal from the water. The EP process is one of them, and in recent years, the number of research works focusing

on EP has increased. The EP method has demonstrated promise in removing hardness without chemical additives and with the least amount of sludge production. However, it's been observed that EP needs sizable cathodic zones to get enough precipitation (Hasson et al., 2011, 2010). A cathode with a large surface area is necessary for application on an industrial scale to achieve adequate performance. Metal cathodes are susceptible to rust and degrade quickly. Due to the aforementioned issues, cathodes must be changed frequently. Due to this, the method is not only challenging to implement but also impractical from an economic standpoint.

A potential innovation in the field of civil engineering is conductive concrete. Recently, the infrastructure for transportation has benefited greatly from electrically conductive concrete (ECON). It is a tried-and-true technique for removing ice and snow from the surface that is structurally reliable. (Sassani et al., 2018; Abdualla et al., 2018; Ceylan et al., 2014; Pan et al., 2015; Sadati et al., 2018). Electrically conductive elements are added to regular concrete mixtures to create these conductive concretes. As conductive materials, carbon fibers, steel shavings, and graphite powder are mixed with concrete. (Notani et al., 2019, Sassani et al., 2017, Arabzadeh et al., 2019) In this study, the concrete was made conductive using graphite powder. This is a unique technique in which an electrochemical precipitation system uses conductive concrete as the cathode.

CHAPTER II

LITERATURE REVIEW

In this chapter theoretical background of electrochemical precipitation and latest progress in the field of electrochemical water hardness treatment has been discussed.

A pair or multiple electrode setup, treatment water, and a DC power source make up a typical electrochemical precipitation cell. In a typical EP configuration, both electrodes are submerged in water (Fig. 2). The cathode's role is to produce alkalinity and serve as the surface where scale is deposited. The separation of anodic and cathodic environments requires no intermediary. To encourage precipitation as a thin layer close to the cathodic surface, a high pH condition is required. As a result, only the thin water film next to the cathodic surface experiences the precipitation reaction (Tlili et al., 2003b, 2003a).

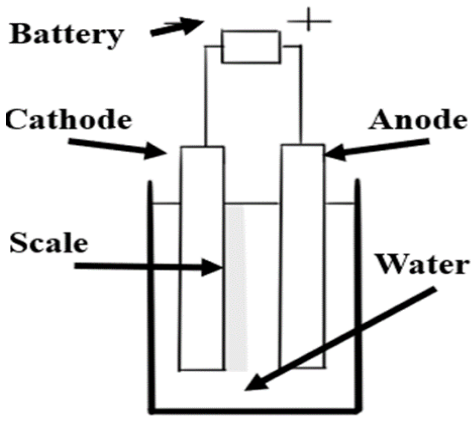

Figure 2: Electrochemical precipitation

During water electrolysis, dissolved oxygen is reduced on the cathode in a large potential range. A basic environment near the cathodic surface is created by the following cathodic reactions (Gabrielli et al., 2006; Kalash et al., 2015b):

$$O_2 + 2H_2O + 4e^- \rightarrow 4OH^- \quad (1)$$

$$2H_2O + 2e^- \rightarrow H_2\uparrow + 2OH^- \quad (2)$$

The reaction rate is not limited by mass transport, and the current intensity can be very high (Gabrielli et al., 2006).

The hydroxyl ion generates either by (1) or (2) and starts to destabilize the Calco-carbonic equilibrium of the solution (Legrand et al., 1981). The high alkaline environment converts HCO_3^- ions into carbonate ions by the following reaction:

$$HCO^-_3 + OH^- \rightarrow CO_3^{2-} + H_2O \quad (3)$$

In the next step, carbonate ions react with calcium ions to start the nucleation and create CaCO3 crystals by the following reaction:

$$Ca^{2+} + HCO_3^- + 2OH^- \rightarrow CaCO_3\downarrow + H_2O \quad (4)$$

$$Mg^{2+} + 2OH^- \rightarrow Mg(OH)_2\downarrow \quad (5)$$

The rate of hydroxyl generation is directly related to Faraday's law. Hydroxyl generation (R_{OH} mole/s) is proportional to i ampere, and the following equation describes it. (Eq. 6)

$$\frac{i}{F}\eta = R_{OH} \quad (6)$$

Where F is Faraday constant (96,485 coulombs/mole), and η is the current efficiency of the ratio of moles CaCO3 precipitated to a specific hydroxyl ion mole.

These particular hydroxyl ions are produced by the current flowing. Both cathodic and anodic reactions in the EP process are governed by the current density. The relationship between current density and the quantity of dissolved metallic electrodes is described by Faraday's law. (Eq 7) (2010) Comninellis and Chen (Wang et al., 2002; Aguilar et al., 2005)

$$n = it/zF \quad (7)$$

Where t is the electrolysis operation time in seconds, F is the Faraday constant, and z is the charge of the cation (Martnez-Huitle et al., 2018) and n is the number of moles of metals dissolved.

Recent research progress in electrochemical hardness removal from water can be divided into four parts.

Softening of tap water

Because brackish water is more conductive (50 mS cm-1) than seawater (0.5 mS cm-1), it is more advantageous to remove hardness from brackish water using the EP method (Clauwaert et al., 2020). However, a few studies have documented some successes. (Kalash et al., 2015b) used the EP method to remove calcium carbonate-containing hardness from municipal tap water, which had a hardness of 330 mg/L. They were able to remove roughly 85% of the hardness. The electrodes utilized in this experiment were aluminum cathodes and graphite anode plates. In Campina Grande, Paraiba State, Brazil, (Agostinho et al., 2012) achieved 80% hardness reduction from tap water with beginning hardness of 355 mg/L as calcium carbonate. In 40 minutes of treatment, these results were achieved using steel and aluminum electrodes.

Treatment of cooling water

Cooling water is a medium used in industrial applications to reject extra process heat (Song et al., 2018). A cooling tower and the piping surrounding it make up an evaporative cooling water system (Becker et al., 2009). Hardness ions scaling in the circulation system is caused by cooling water evaporation. This characteristic makes water softening crucial, especially for industrial uses, when using water for cooling. In industries, it's usual practice to combine softened water with cooling water to keep the overall hardness under 400 mg/L due to CaCO3 (Moran, 2018). In hard cooling water, (Yu et al., 2019) increased total hardness removal efficiency up to 21.6% using a multistage

electrochemical precipitation reactor. (Luan et al., 2019) used a multi-mesh system to successfully lower the test solution's total hardness from 350 mg/L of CaCO3 to under 100 mg/L of CaCO3 from a Chinese manufacturing company in Shan Dong. The removal of total hardness up to 22.8% was tested by (Yu et al., 2018a) using a lab-scale batch hardness removal device. Yu et al. (2018b) achieved a final overall hardness reduction efficiency of 12.2 to 15.2% in separate research. (Jin et al., 2019) used titanium DSA (Dimensionally Stable Anode) as both the anode and the cathode in the EP process to achieve a total harness removal efficiency of 16.4–21.4% from cooling water. Additionally, the EP process with a high-efficiency multi-layer mesh linked cathode was evaluated by (Li et al., 2020). The study's findings suggested that internal and external layers worked together to improve performance, which suggests that the cathode area requirement of the EP system may eventually be exceeded.

Descaling the cathode surface

Preventing scaling on the cathode surface is one of the major issues facing the EP system. A comparison between several descaling techniques is presented in Table 1. The search for a more effective descaling technique for the EP process has seen a substantial increase in research. Pulsating current was suggested as a unique technique by Yu et al. (2018) during the EP process. The study demonstrated that higher gas pressure on the crystals linked to the cathode was caused by increased current density. Higher descaling was consequently seen (Table 2). The connection between turbidity and current density is explained. The paper also asserted that it was feasible to undertake repeated descaling operations without degradation. Yu et al(2018b) 's suggestion for

descaling the cathode involved air-scoured washing. This technique has primarily been used for filter backwashing (Liu and Liu, 2016; Park et al., 2016). It was found that the performance of the scale detachment was primarily affected by the airflow rate per unit cathodic area. According to the study, air scoured cleaning holds promise as a descaling technique. Polarity reversal was used by (Jin et al., 2019) to descale the cathode. In numerous technologies, including electrode ionization and electrodialysis, this descaling technique has been demonstrated to be effective (Lee et al., 2006; Valero and Arbós, 2010; Yeon et al., 2007). Descaling begins when the electrodes' polarity is flipped since this causes the electricity's poles to shift. A higher descaling rate during polarity reversal was shown to be the outcome of the increased current density during polarity reversal, according to an experimental finding.

Table 1: Comparison of different descaling techniques (Yu et al., 2018b)

Descaling Technique	**Advantages**	**Drawbacks**
Mechanical Scraping	Easily operational	Low softening efficiency and high energy consumption
Polarity Reversal	Simple configuration	Costly and environmentally harmful
Acid Washing	High detachment efficiency	Severely reduced electrode lifetime
Ultrasonic	Satisfactory descaling efficiency and environmental friendliness	Complicated configuration, difficulty in maintenance
Air-Scoured Washing	Simple configuration, easy operation	Require a separate air supply system

Cell design and process improvement

Recently created revolutionary softening techniques include better cell designs and process improvements. By addressing one of the most pervasive issues with EP, a lack of cathodic surface area, the majority of these techniques improved hardness removal over the predecessors. (Luan et al., 2019) used a multi mesh structure rather than single cells to improve the active cathodic surface area. Eight cells made up a multistage EP reactor that was tested by (Yu et al., 2018a). The multistage device demonstrated superior water softening efficacy to the traditional ways while using comparably less energy. When ordinary unsalted water was treated, a larger ohmic drop was seen from the same multilayer system. (Yu et al., 2018b) combined cathode and anode electrochemical cell compartments with ion-exchange membranes in between. The process eliminated 40–44% magnesium and 73–78% calcium. Sanjuana et al. (2019) used a novel 3D stainless steel woolen cathode under different experimental conditions. The results showed that the 3D electrode has a higher electrode area, leading to greater hardness removal efficiency and lower energy consumption compared to conventional 2D electrodes. Zhi *et al.* (2016) used a novel electrochemical system that employed both conventional EC and EP processes. The EC process removed hardness ions by scale precipitation and adsorption of Ca^{2+} and Mg^{2+} to the $Al(OH)_{3n}$ floc produced from Al anode surface (Z. Liao *et al.*, 2009).

Factors affecting electrochemical precipitation

Water hardness can be removed by applying electric power to cathode and anode submerged in the hard water via. This process is called electrochemical water treatment (Gabrielli *et al.*, 2006; Malakootian *et al.*, 2010; Hasson *et al.*, 2008). Electrochemical precipitation (Luan *et al.*, 2019; Xinhao Li *et al.*, 2020) is one of the recent developed electrochemical water treatment processes that has shown a good potential in removing water hardness efficiently. In this process, the hardness is removed by forming an alkaline environment and depositing precipitates of soluble metals around the cathode (Agostinho *et al.*, 2012; Henry A. Becker *et al.*, 2009; Caluwaert *et al.*, 2019). Research on this water hardness removal technique has been done in the laboratory as both batch and continuous flow conditions as shown in Table 2.

Table 2: Current Density, Cell Voltage, Hardness removal efficiency

Paper Author Name	Electrodes used	Distance between cathode and anode	current density (A/m^2)	Feed solution	Flow rate	Reactor	Removal Efficiency
AGOSTINHO ET AL (2012)	Anode- Aluminium sheet Cathode – Steel sheet	0.5 cm		Tap water		Batch	80%
Becker *et al.* (2009)	Anode – titanium coated with Iridium oxide Cathode – Stainless steel mesh		7-10	Tap water	18L/hr.	Continuous	86 – 73% (Calcium removal Efficiency)
Emamjomeh *et al.* (2009)	Cathode and anode - Aluminium	5 mm	12.5-50 A/m^2	Synthetic tap water	150-400 mL/min	Continuous	fluoride removal efficiency-89-99%
Gabrielli *et al.* (2006)	Cathode - stainless steel plate Anode - titanium cast iridium oxide	15-40mm	4-20 A/m^2	Tap water	1.68-12 L/hr.	continuous	66 % for detention time 1 hr.
Hasson *et al.* (2008)	Cathode- Stainless steel Anode – DSA (titanium alloy)	11 mm		Synthetic water	1 L/min.	Continuous	

In a continuous flow condition of the EP process, several experimental parameters can affect the hardness removal efficiency, precipitation rate, and specific energy consumption, which include:

Flow rate

The flow rate has a significant impact on hardness removal, precipitation rate, and energy consumption. S.H. Lee *et al.* (2002) found that the increase in the flow velocity and the decline of the retention time causes insufficient diffusion of the scaling ions close to the cathode surface, which resulted a gradual reduction in the hardness removal rate. According to Luan *et al.* (2019), precipitation rate increased due to the mass transfer of hardness causing ions around the cathode as flow rate is increased to a critical flow rate value (400 L/hr.) in a continuous flow reactor of the multi-meshed cathode setup at a flow rate greater than critical rate, hardness removal efficiency dropped (Emamjomeh *et al.*, 2009). Increased flow rate decreased specific energy consumption per *Hasson et al.* (2008), thus making the EP process more favorable. The effect of flow velocity on the specific energy consumption and the $CaCO_3$ deposition rate was explored over the range of 0.5 to 2.5 L/min.

Applied voltage and current density

The hardness removal rate directly relates to the current density (Yu et al., 2019). The increased current density and voltage make bubbles in treated water-dense and smaller. It increases the active surface area of the bubbles, and greater flotation efficiency can be achieved. This all leads to an increased OH^- production (Table 3) (Clauwaert et al., 2020) and greater hardness removal from the water.

Table 3: Change of hydroxyl production with charge density (Clauwaert et al., 2020)

Charge Density (C L^{-1} tap water)	**Hydroxyl production (mmol OH^- L^- tap water)**
175	181
524	543
1097	1137
2237	2318
3129	3243

Electrode Material

For all electrochemical processes, the electrode material is essential. For best performance, the electrode material must meet the following criteria: (a) Physically and chemically very stable; (b) High electrical conductivity; and (c) Low cost/life ratio (Chen, 2004; Angelada et al., 2009). The electrodes' materials can alter both the electrical efficiency and the effectiveness of removing hardness. Table 4 illustrates the significance of electrode material. The treatment water's original hardness was 350 mg/l as CaCO3 (Yu et al., 2018).

Table 4: Effect of electrode material on hardness removal (Yu et al., 2018b)

Calcium Removal (mg/L)	**Titanium**	**Nickel**	**Normal Stainless Steel**	**Frosted Stainless steel**	**Mirror Stainless Steel**
1st trial	46.06	54.14	55.75	53.65	61.15
2nd trial	48.48	51.71	54.94	53.33	62.22
3rdtrial	45.25	52.52	54.14	50.10	59.48

Inter-electrode distance

Hardness removal efficiency drops at a greater inter-electrode distance. Energy consumption also increases as the voltage increases in the EP system at a greater inter-electrode distance. At the same electrolysis time of 10 mins, the hardness removal rate decreases as the inter-electrode distance increases. The reason is that the smaller the electrode distances are the larger the contact area between the solution and the plates. It results more electrochemical reactions and improved the chemical reaction rate. (Wang & Zhang *et al.*, 2019) In most of the EP setups, the electrode distance was taken between 0.5-2 cm for the optimum results. (Khairi *et al.*, 2014; Gabrielli *et al.*, 2006).

Effect of retention time

The retention time affects the rate of calcium and magnesium precipitation. When pH and potential difference are constant, electrolysis time is directly proportional to the amount of hardness removed (Yu et al., 2018b). discovered that for the first four minutes of the experiment, electrolytic hardness reduction and hydraulic retention time were directly proportional (Fig. 3).

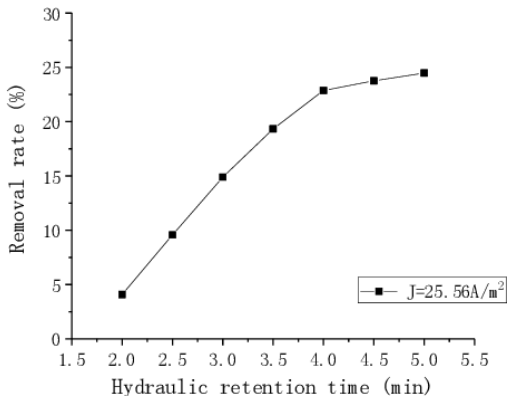

Figure 3: Effect of retention time (Yu et al., 2018b)

CHAPTER III

OBJECTIVES

This study aims to develop a lab scale electrochemical precipitation cell using graphite concrete electrodes.

- Determining whether a cathode made of graphite concrete will work in an electrochemical precipitation cell. The goal was to use an effective amount of graphite in the concrete to minimize resistivity as low as possible.
- Putting together a functional lab scale system. This includes determining the best settings for the most output, the best power sources, and safety procedures.
- Selecting the setup's optimal operational variables. It is important to carefully test the effects of Current density, flow rate and reaction time variation.
- Effect of continuous electrochemical precipitation on the quality of the water after softening.
- Determining the experimental setup's maximum hardness removal capacity.

CHAPTER IV

METHODOLOGY

Conductive Concrete

The chosen mold size was 76.3 mm×17.77 mm× 20.33mm. The coarse aggregate size was #8 no sieve passing and containing maximum and minimum sizes of 9.5 mm and 2.38 mm respectively. Fine aggregate of #8 sieve passing and #100 sieve retaining was used (Fig 4). Water cement ratio of 0.45 and air content of 4.5% was used. Additional natural flake graphite powder was used to make the concrete conductive. The physical properties of the graphite are shown in the Table 5.

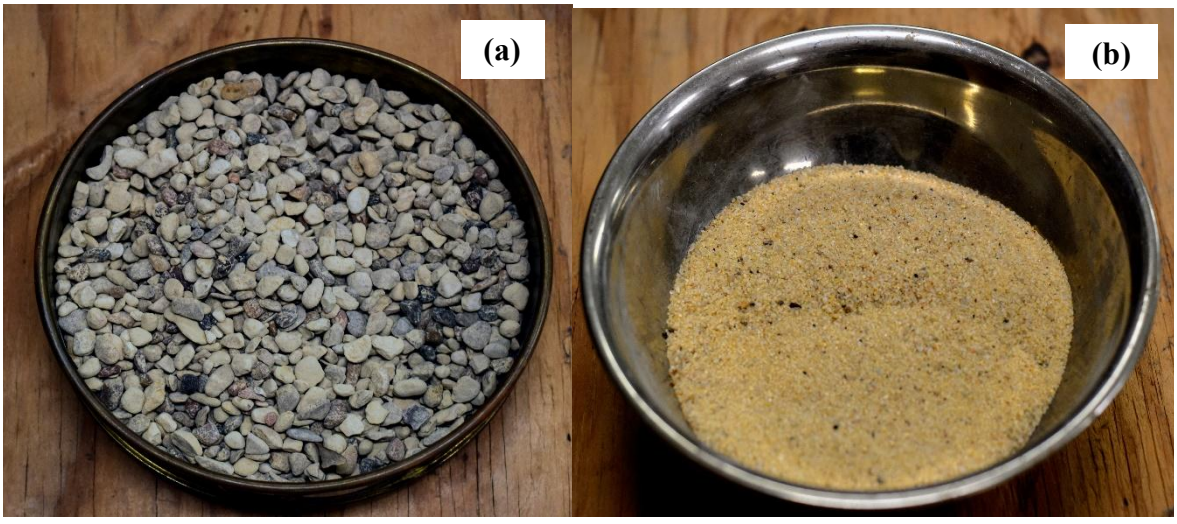

Figure 4: a) Coarse Aggregate b) Fine aggregate

Table 5: Physical Properties of the natural flake graphite powder used in experiment

Percent Carbon	Typical Size (μm)	Specific Gravity	Surface area (m^2/g)	Typical Resistivity (Ω-cm)	Note
95.46%	50-60	2.6	5	0.03-0.05	Flake

Graphite was added to the concrete mix of cement, coarse, fine aggregate, and water homogenously. Specimens were cast containing 10% graphite powder. The specimens were cast according to the standard ASTM methodology. Mix design of graphite conductive concrete cathode used in this experiment are shown in Table 6.

Table 6: Mix Design of Graphite Concrete Cathodes

Materials	Mix Design of 10% graphite concrete (gm)
Water	25
Cement	55.55
Coarse Aggregate	105.838
Fine Aggregate	127.46
Graphite	31.14

The inside of the molds was well lubricated with grease and the molds were reinforced with wooden pieces. The concrete containing graphite was poured into the mold in three layers. The

cast specimen was kept in room temperature of 25℃ for 24 hours. After the concrete was set, it was kept under water for curing for 14 days.

Preparation of the specimen

Cured specimens were towel dried and followed by submerging them in water again for a minimum of 24 hours. This would cause the concrete to be saturated which would simulate similar conditions to a concrete pipe or reservoir. After that the saturated concrete specimen was then coated with PELCO conductive nickel paste (Tedpella, USA) (Fig 5). This nickel paste was from Tedpella USA and contain pure nickel flakes (8-15 μm). This paste was used to create a thin, conductive and flexible layer on the conductive concrete specimen. This paste is more conductive than other paints such as of graphite or silver. On this nickel paste conductive copper tape is wrapped. This tape is made with copper foil with an acrylic conductive adhesive.

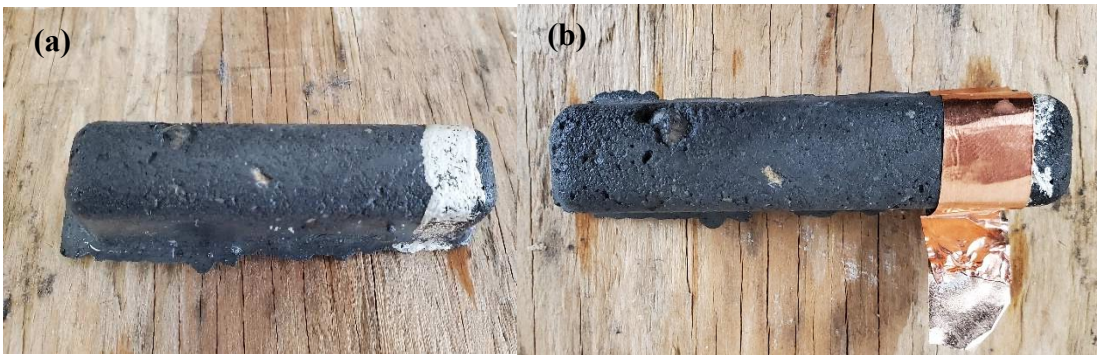

Figure 5: a) Applying nickel paste on conductive concrete cathode b) Applying copper tape over the nickel paste in this experiment

Treatment water

The water used in the experiment was tap water. The source was environmental engineering lab in UTRGV Edinburg campus. Before collecting sample water, the water was kept running for 10

mins. Water was collected in 1 liter glass beaker. The initial hardness of the sample water was between 290-300 mg/L as $CaCO_3$. Initial pH was 7.2 on average. The temperature of the water was 23 degrees.

Experimental Setup

The experimental setup, shown on Figure 6 and 7, was completed by connecting the anode and cathode with a DC power source which consisted of a maximum voltage of 31 V and current of 5 A. Both of parameters can be regulated as per required. Anode and cathode were placed vertically in the reactor with a specified distance between them. Dimensionally stable anode (DSA) was used as anode and conductive concrete was used as cathode. DSA anodes were 2" by 6" in dimension. 18 -gauge wire and claps were used to connect the electrodes with the power supply. 1 litre beaker was used an electrochemical reactor. Finally, a peristaltic pump was added to continuously add water into the reactor. It was made sure the electrodes were submerged as much as possible. This allowed a maximum surface area efficiency. After reaching the pre-determined hydraulic retention time, it would overflow out of the reactor and not return to the beaker, so as to better simulate the actual situation. The function of the graphite concrete cathode was to generate alkalinity and be the scale deposition surface. No medium was needed for the separation of anodic and cathodic environments. The high pH condition was necessary to promote precipitation near the cathodic surface as a thin layer. As a result, the precipitation reaction occurred exclusively in the thin water film adjacent to the cathodic surface (Tlili et al., 2003a, 2003b).

Figure 6: Placement of electrodes in experiment.

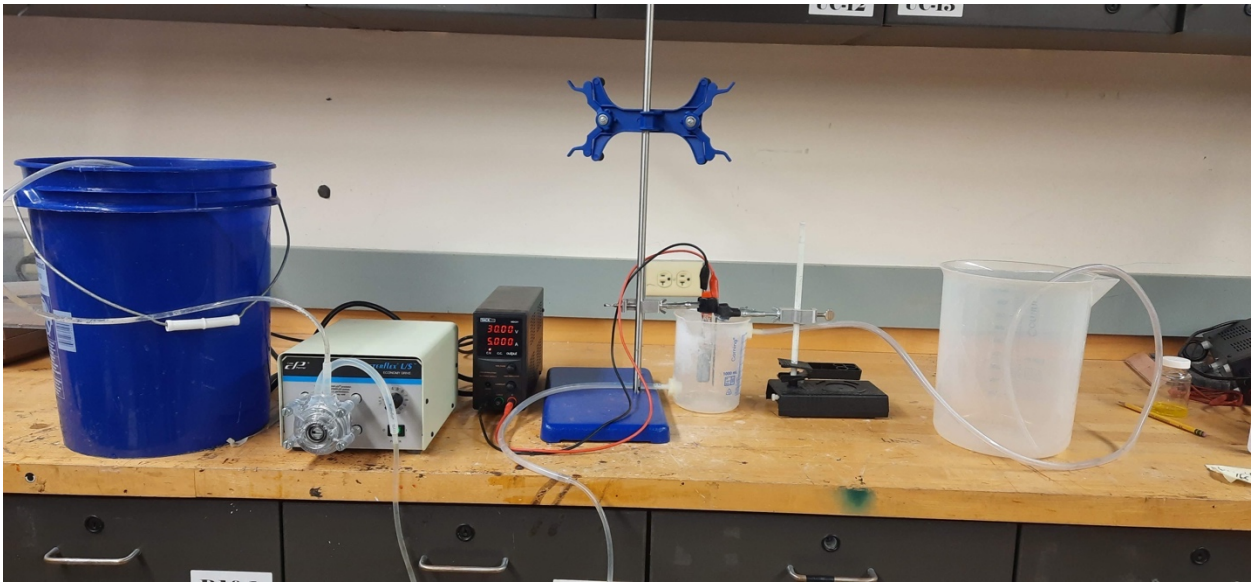

Figure 7: Experimental setup.

In this experiment, the effect of current density, flow rate (hydraulic retention time), pH, treatment time on hardness removal had been investigated. The experiment was conducted to collect to samples at 15mins. interval with a constant voltage of 30 V and a variable current and

flow rate value. The cathode was made up of concrete with 10% graphite content of the total volume.

Before conducting each experiment initial pH, Hardness, alkalinity, total dissolved solids (TDS) and temperature was recorded. After specified treatment time, treated water precipitation was removed by filtering through the 1 μm glass fiber filter connected to vacuum filter (WELCH 2534B-01A, Louisiana, USA). Then the pH, hardness, alkalinity, TDS and temperature was measured again. the hardness of water was checked with EDTA (Ethylenediamine Tetraacetic Acid) titration method according to the standard method. After that pH multimeter HACH HQ40d (HACH, Colorado, USA) was used to measure the initial pH of water. Following that LaMatte Alkalinity DRT kit was used to measure the alkalinity of the water.

Three sets of cylindrical specimens containing 5%, 7.5%, and 10% graphite were created to measure the compressive strength of conductive concrete. Each set had three samples. The cylindrical mold had a diameter and height of 10 and 20 cm, respectively. Concrete with a graphite content was poured into the mold, and the empty area between the concrete was eliminated by compacting the concrete. The entire casting process was carried out and kept up to ASTM standards. Specimens were removed and submerged in water for 28 days of cure after a 24-hour casting period. The specimens were given the names 10 T1, 10 T2, and 10 T3 for 10% graphite concentration, 7.5 T1, 7.5 T2, and 7.5 T3 for 7.5%, and 5 T1, 5 T2, and 5 T3 for 5%. (Figure 8).

For this known standard, ASTM C39M-21 was used. The compressive strength test was conducted using a Forney F250 compressive strength machine (Forney Corporation, Texas, USA). Weight was determined for input using a common scale equipment. The specimen was

placed between the pistons that provided the load (Fig 9). To ensure that debris wouldn't hurt the experimenters or the machine, safety precautions were adopted. When the specimens had a visible crack and the highest compressive strength had been recorded, the loading was halted. (Fig 10)

Figure 8: Conductive concrete cylinders containing 10% graphite by volume. Specimens are 10 cm by diameter and 20 cm by length. (a) side view of the specimens and (b) top view of the cylindrical specimens.

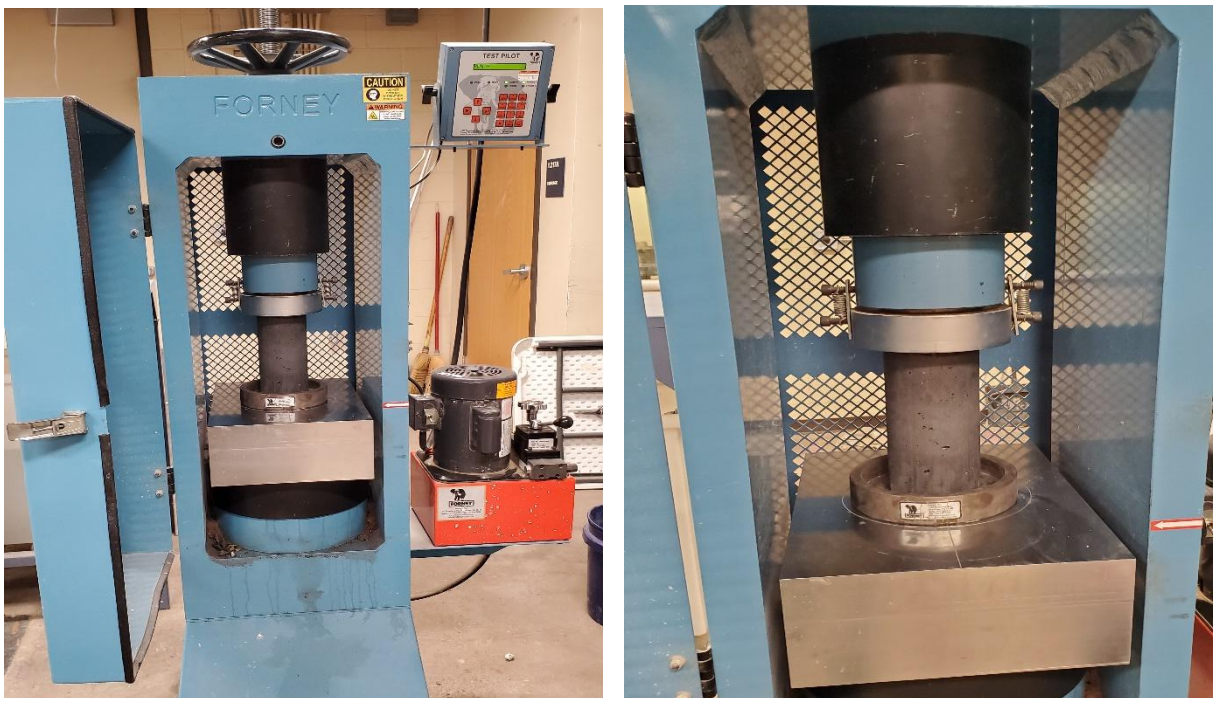

Figure 9: (a)Conducting compressive strength test on FORNEY F250. (b) specimen setup for the compressive strength test.

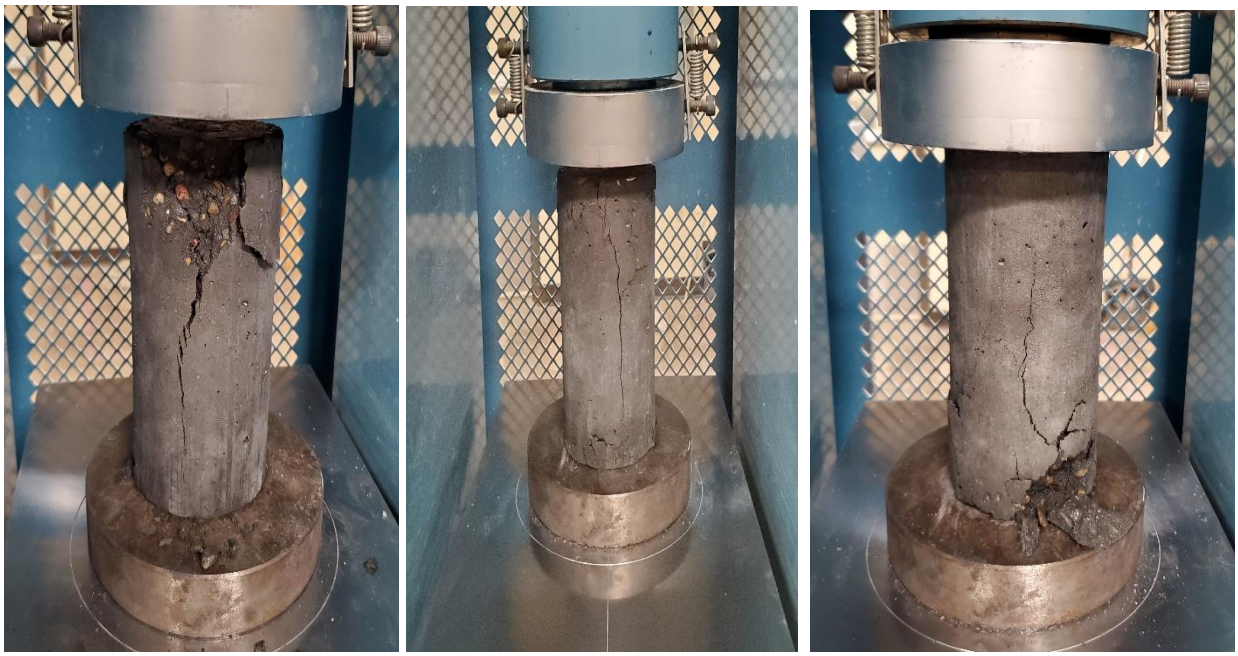

Figure 10: Failure of specimen 10T1, 10T2 and 10T3 under lateral loading

Three sets of cubical specimens with graphite contents of 5%, 7.5%, and 10% were created using the same concrete mix design for compressive strength in order to measure the resistivity of the conductive concrete. The specimen measured 2 inches by 2 inches by 2 inches. Specimens were bonded using copper tape, nickel paste, and polyethylene paper to maintain a steady moisture level after 28 days of curing (Fig 11). The impedance spectrometer is then used to measure impedance.

Figure 11: Specimens for impedance measurement.

Several parameters are entered before the measurement (Fig 12). The maximum integration time was 0.25, the maximum number of cycles was 10, the amplitude threshold was 5%, the steady state was reached after 10 cycles, the highest resolution was 32, and the maximum amount of measurement was 25. Using an impedance spectrometer, the Bode plot, Nyquist diagram, and resistance reading were measured.

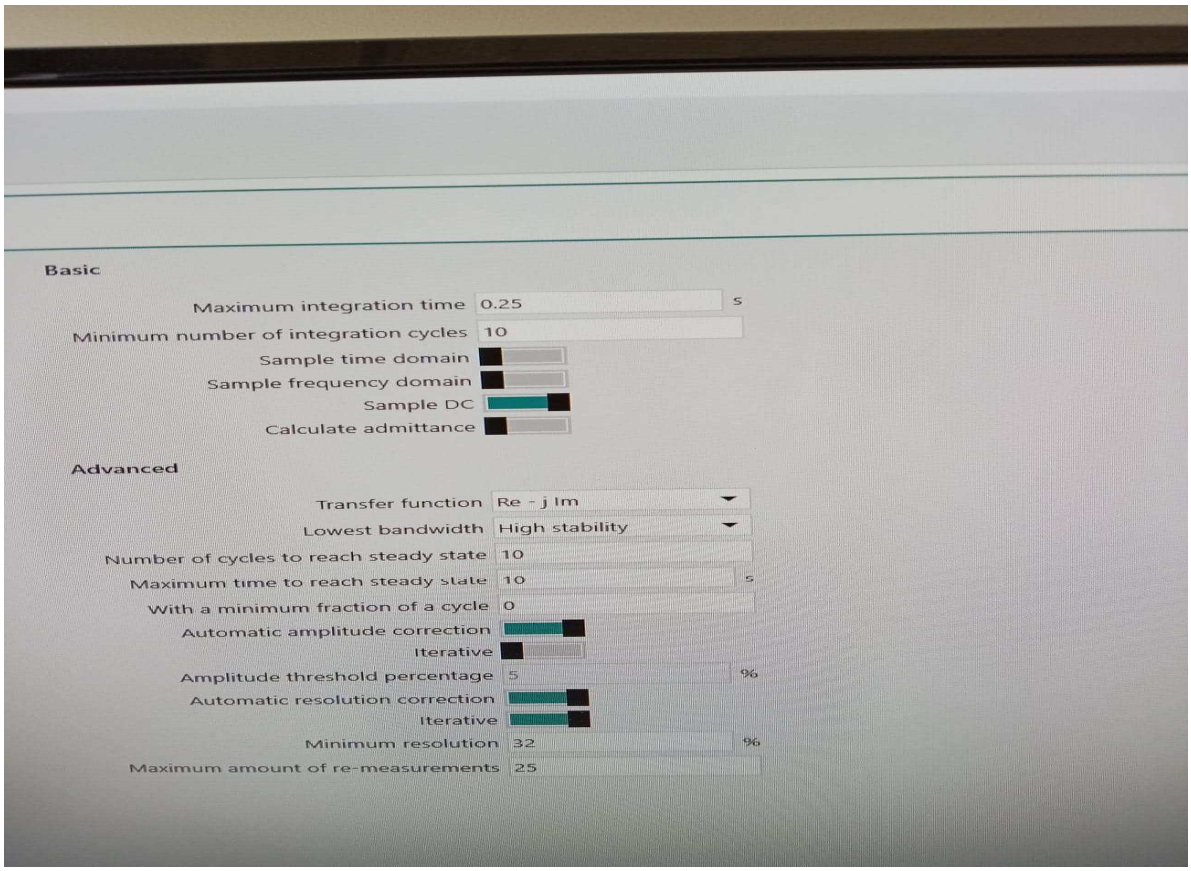

Figure 12: Basic input parameter before impedance measurement.

CHAPTER V

RESULTS AND DISCUSSION

Resistivity

Impedance spectroscopy (IS) was used throughout the experiments to measure the electrical properties of specimens. Using Alternate Current (AC), four pieces of information have been collected- real impedance, imaginary impedance, impedance, and phase angle. These information has been used to draw three graphs containing Nyquist Diagram, Bode Plot impedance and Bode Plot Phase angle diagram. Nyquist diagram has been drawn plotting real impedance in X-axis and imaginary impedance in Y-axis while bode plot impedance has been drawn plotting frequency in horizontal and impedance in vertical and bode plot phase angle has been drawn plotting frequency in horizontal and phase angle in vertical.

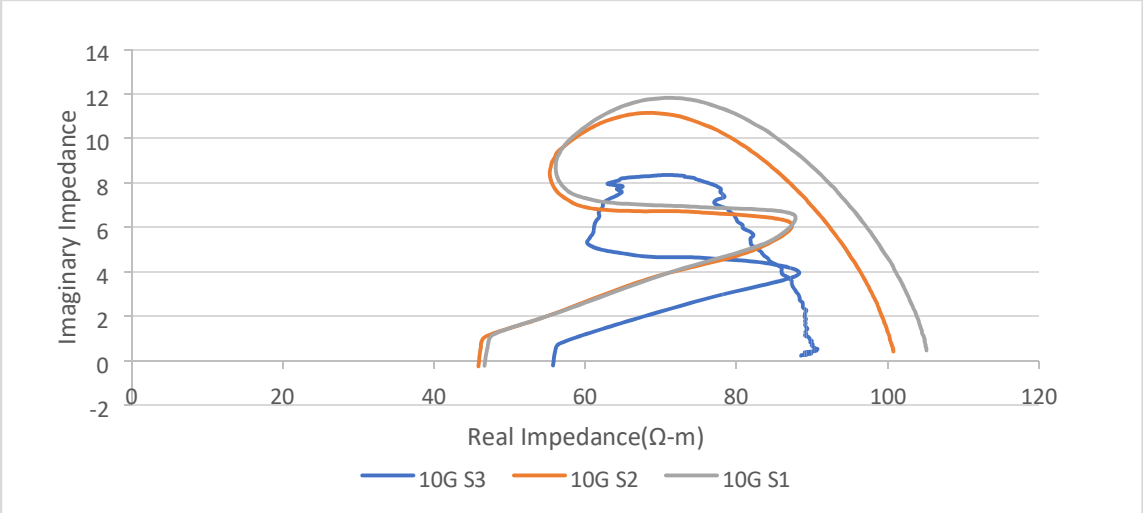

Figure 13: Nyquist diagram for 10 percent graphite

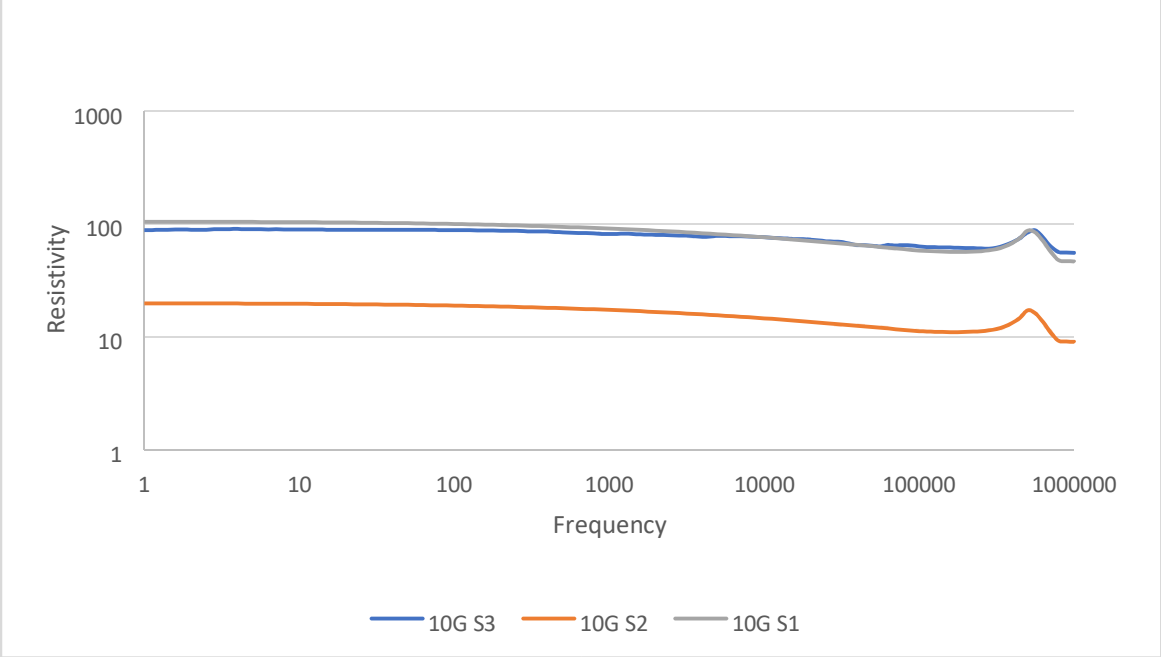

Figure 14: Bode plot diagram for 10 percent graphite

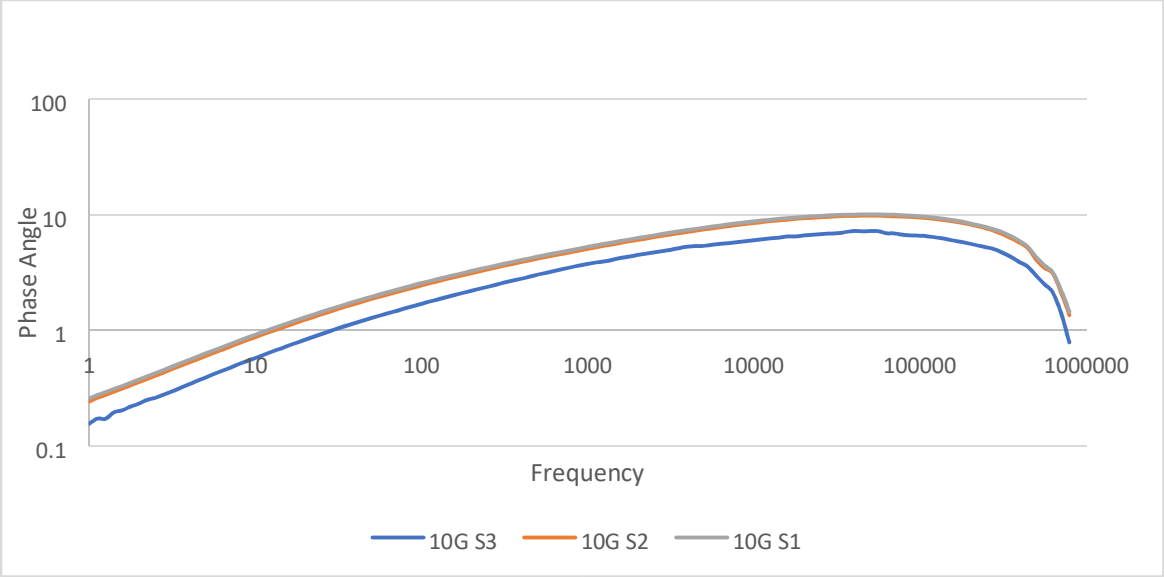

Figure 15: Phase angle diagram for 10 percent graphite

No significant difference was found in Impedance for 10 percent of graphite and 7.5 percent graphite. In 10 percent of graphite, impedance is slightly lower then 100 Ω.cm (Figure 14) and in 7.5 percent of graphite impedance is slightly above of 100 Ω.cm (Figure 17). Nevertheless, both specimens are conductive enough to pass the electricity. The rate at which impedance decreases, slows down at higher frequency which expresses that the materials have some capacitance effects but it is negligible.

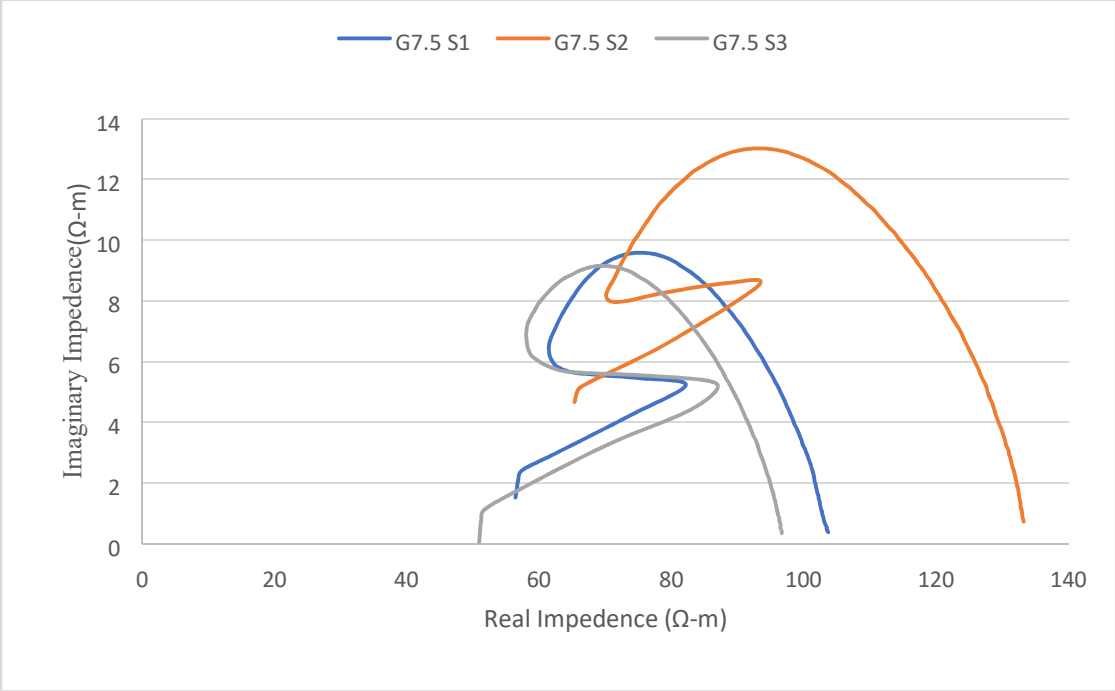

Figure 16: Nyquist diagram for 7.5 percent graphite

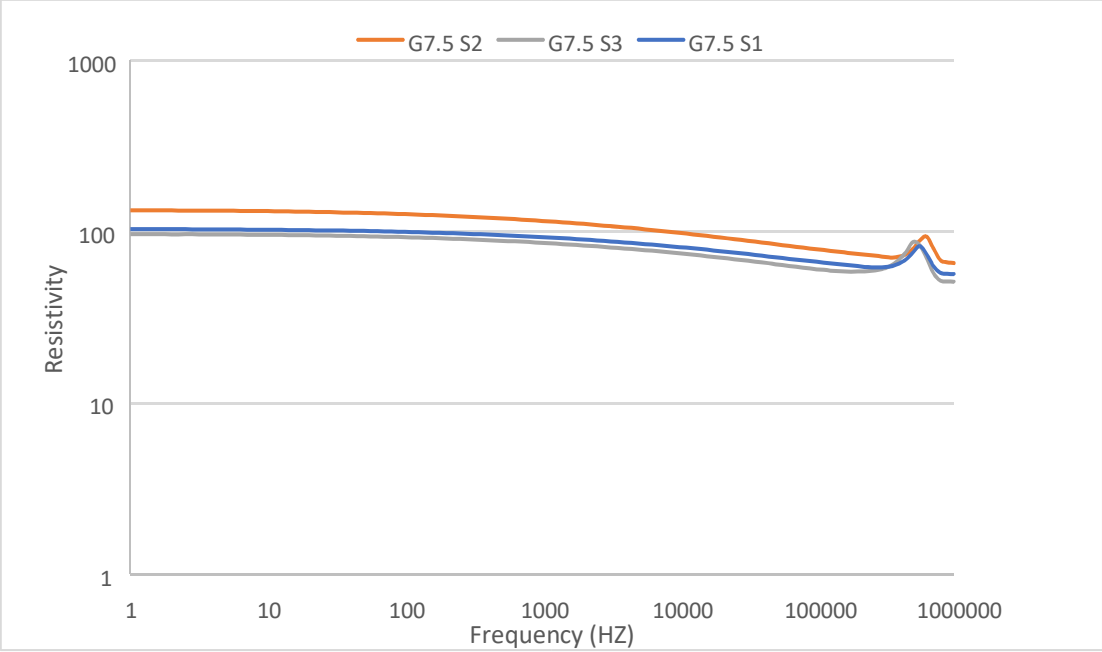

Figure 17: Bode plot diagram for 7.5 percent graphite

It is very tough to explain the Nyquist diagrams for 10 and 7.5 percent of graphite as they are showing too fluctuations (Figure 13 and 16) but graphs for 5 percent of graphite containing concrete are semicircles (Figure 19). The two metal plates which are separated by insular materials behave like a capacitor and materials through which electricity hinders to flow through acts as a resistor. Both of this type of processes is present in cement concrete. The bulk impedance shows semicircle, which means that the capacitor and the resistor are connected in parallel way.

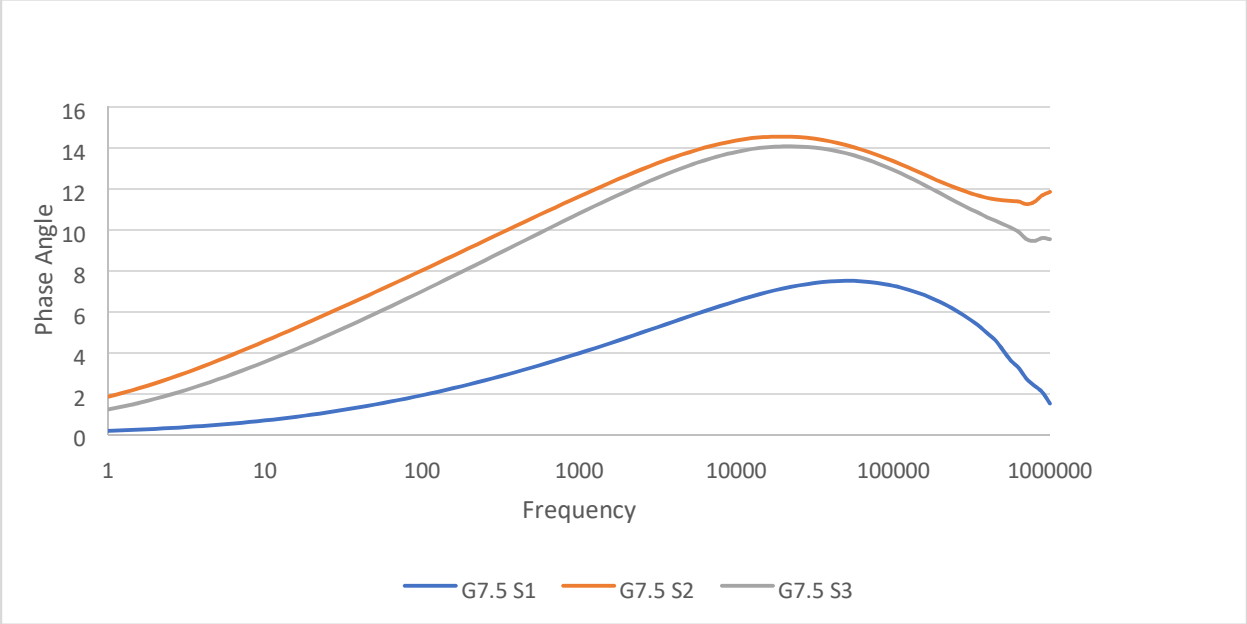

Figure 18: Phase angle diagram for 7.5 percent graphite

For 10 percent and 7.5 percent graphite containing concrete, phase angle starts from almost 0 degree (Figure 15 and Figure 18), and for 5 percent, starts from 5 degree (Figure 20). The phase angle gradually increases with the frequency. A pure resistor would show zero-degree phase angle and the phase angle would increase with the capacitance behavior. In low frequency, the

specimens show no capacitance effects but in high frequency, they show very small capacitance effects.

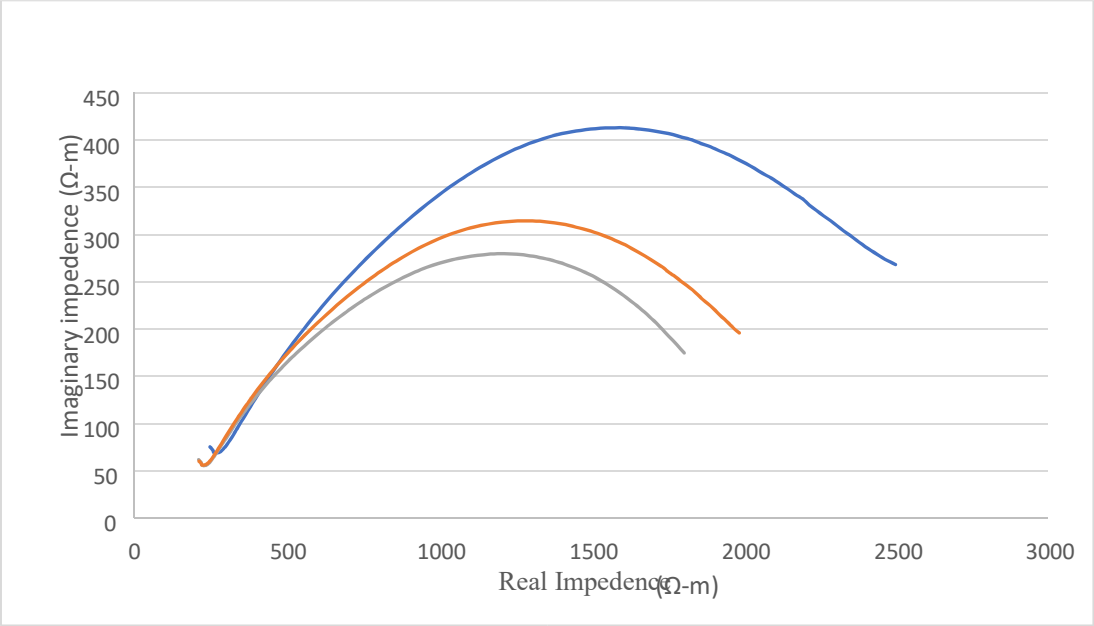

Figure 19: Nyquist diagram for 5 percent graphite

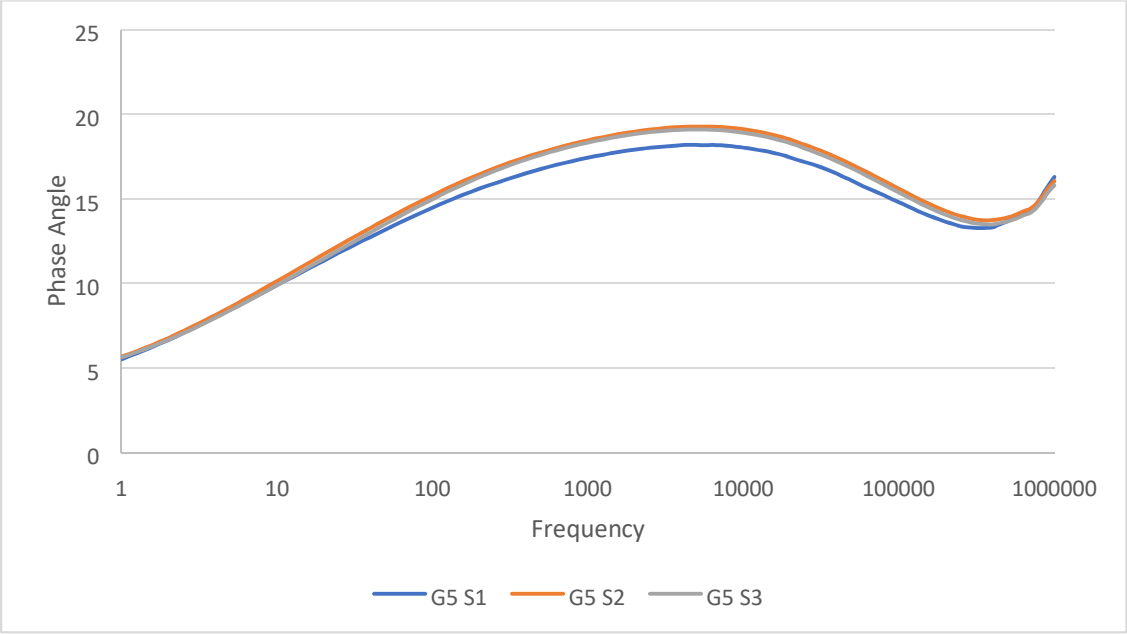

Figure 20: Phase angle diagram for 5 percent graphite

Current density

Electrochemical treatment is greatly influenced by electrical variables (Zhou et al., 2019). The current (i.e., current density) is chosen to represent the electrical parameters since it is more practical to utilize in research and engineering applications than the voltage value. When inputting different current densities, the changes of different indexes in the electrochemical descaling process are plotted in figure 21.

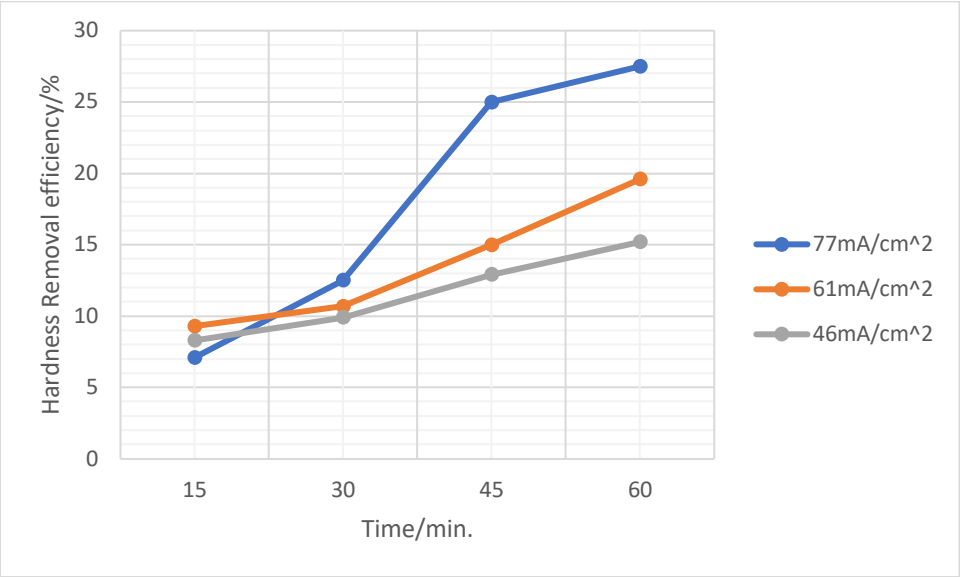

Figure 21: Hardness removal efficiency at different current density.

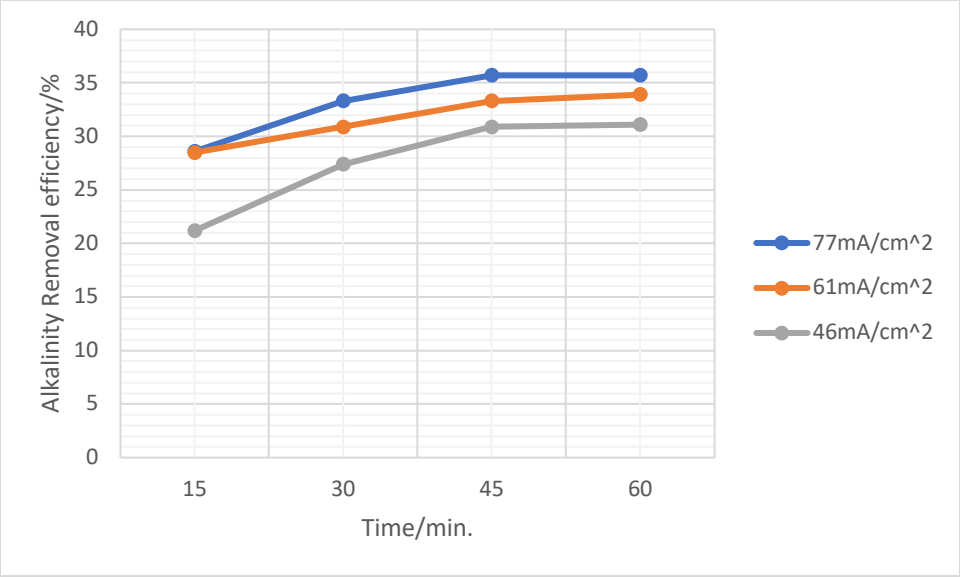

Figure 22: Alkalinity removal efficiency at different current density.

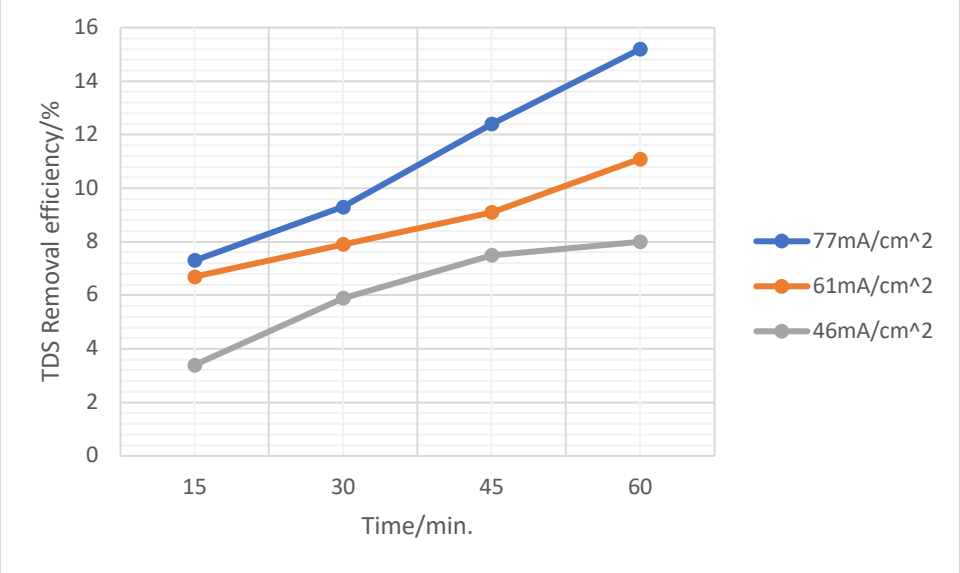

Figure 23: TDS removal efficiency at different current density.

It can be learnt from the figures 21,22, and 23 that hardness, TDS, and alkalinity removal efficiency are closely related to the current density value, and a larger current density value could make the corresponding indexes higher. In this experiment, the best removal rates can be seen for the highest current density value which is 77mA/cm^2. The results were like (Kalash et al., 2015). These results can be explained by the fact that, increasing current density allowed more

electricity to pass through the system. As a result, more electrons could pass through the water at the same time. This process increased the density of the water bubbles adjacent to the cathode, while decreasing the size of them. Since the effective surface and retention time of smaller bubbles were more than the bigger ones, in the same retention time hardness removal efficiency was improved.

Along with having a direct impact on descaling performance, the current density may also have an impact on how the temperature of the electrolyte is affected. According to Fig 24, there is always some degree of temperature rise in the reaction process, independent of the current density value. Ohmic heating is severe at large current densities, creating a noticeable temperature increase. After 60 min. of reaction, when the current density is 46, 61 and 77 mA/cm^2 , the corresponding temperature rise is 6.5, 6.1 and 5.7 degree Celsius.

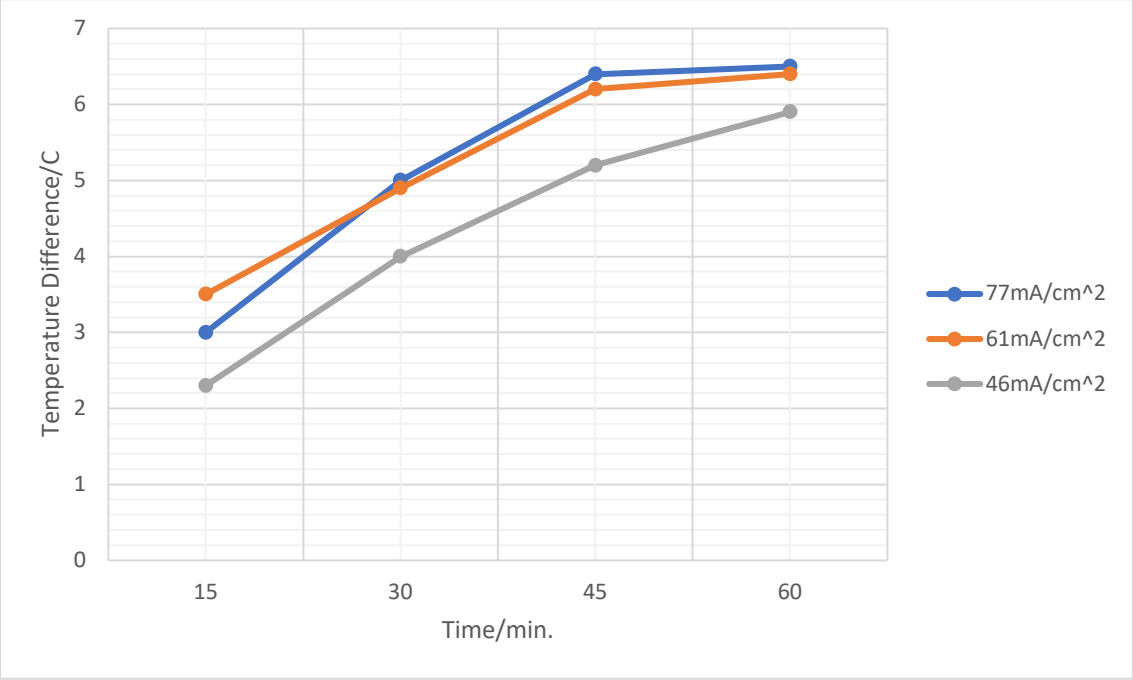

Figure 24: Temperature rise at different current density.

Flow rate

Flow rate is an important parameter to analyze as it affects the hardness removal efficiency in the electrochemical precipitation process. Flow rate determines the hydraulic retention time, which in turn refers the duration for water to remain in the electrochemical reactor (Zu et al., 2020). The larger value presents the longer time for water to participate in the reaction in the reactor and the better treatment performance (San Juan et al., 2019). In this study, four flow rates of 1.5, 3, 5 and 8 L/hr. have been chosen, and their corresponding hydraulic retention times were 40 min, 20 min, 12min and 7.5 min.

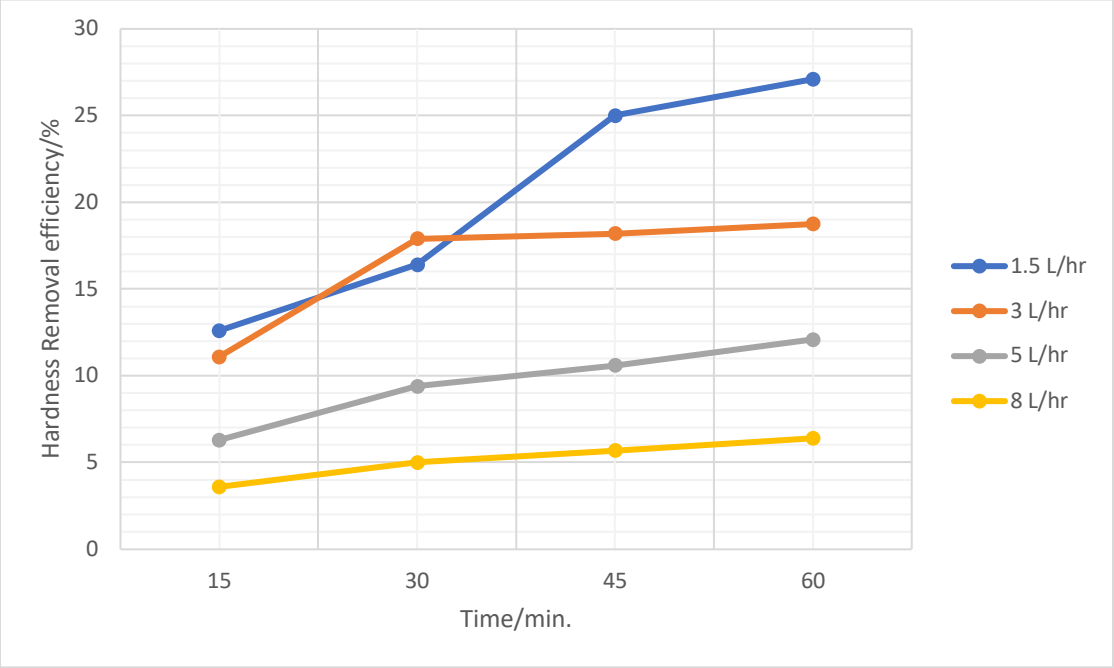

Figure 25: Hardness removal efficiency at different flow rates.

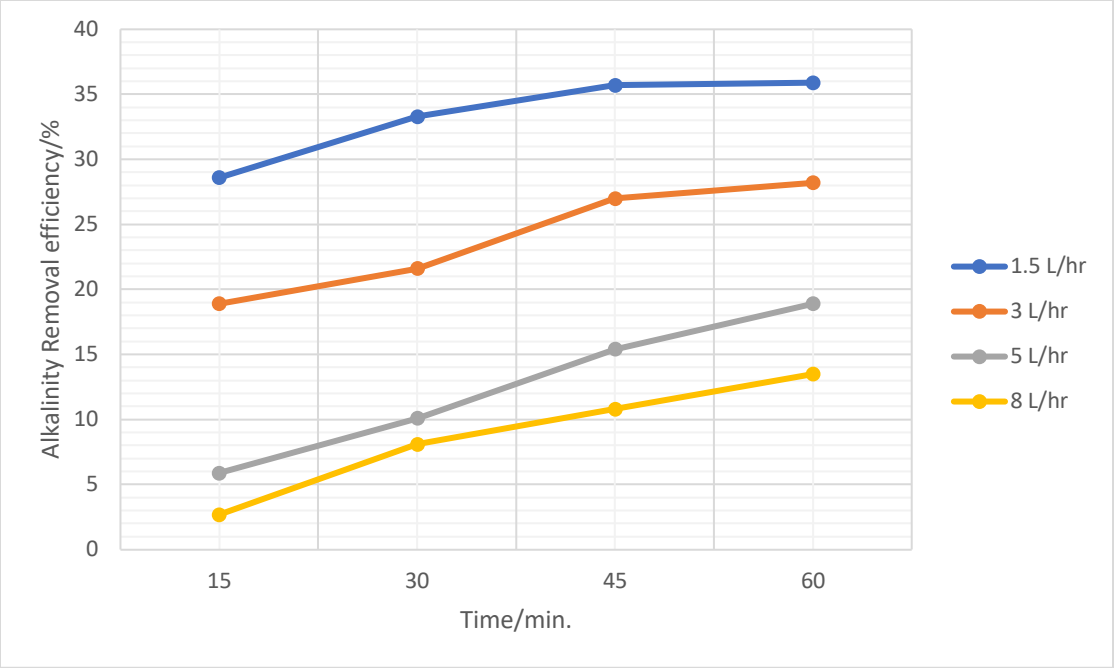

Figure 26: Alkalinity removal efficiency at different flow rates.

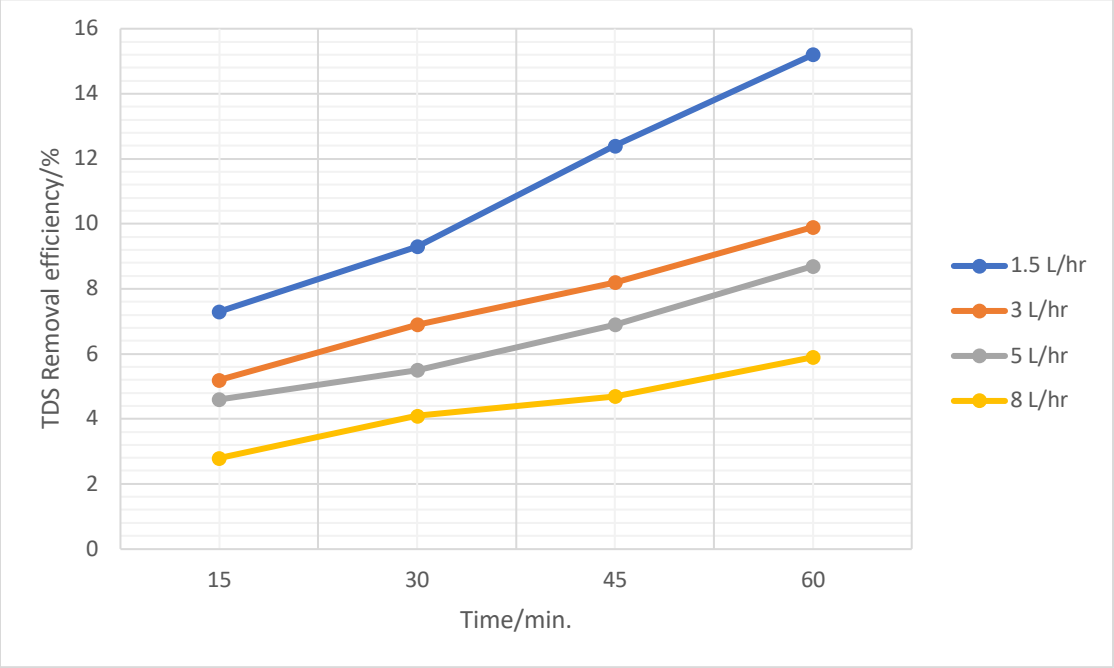

Figure 27: TDS removal efficiency at different flow rates.

The figures 25,26,27, and 28 exhibit the changes of different indexes in the electrochemical descaling process with different flow rates. As illustrated in the figures, hardness, alkalinity, and TDS removal rates all decrease with the increase of flow rates. Low flow rates correspond to high HRT, allowing for adequate water sample treatment in the reactor and longer ohms-based heating times. The flow disturbance condition currently is negligible, which favors the directed migration of Ca2+/Mg2+ to the cathode region and increases the effectiveness of the treatment. On the other hand, a high peristaltic pump (HRT), i.e., high flow rate, speed results in a low HRT, which means that the water sample only spends a short period in the ohmic heating area. So, a change to the water body's steady condition could result in inadequate treatment.

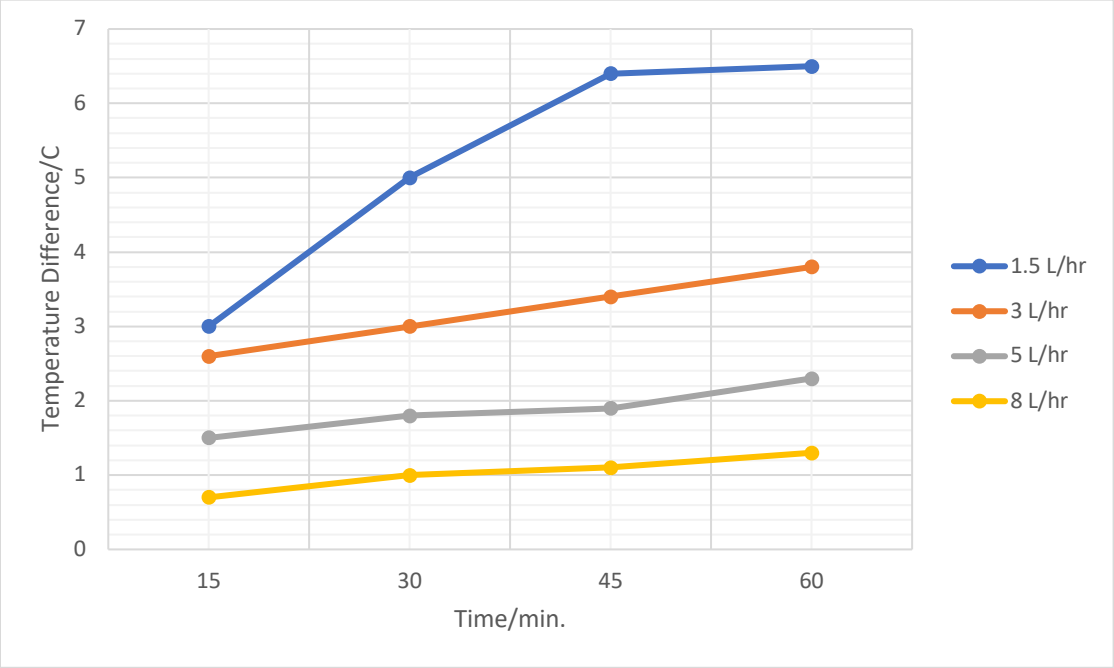

Figure 28: Temperature rise at different flow rates.

This is consistent with the findings of Sung H Lee et al. (2002), who stated that a decrease in the retention time of the solution in the electrolytic cell and an increase in the main flow velocity could result in insufficient scaling ions diffusing to the cathode plate's surface, thereby gradually slowing the rate at which hardness is being removed. Implementing high HRT helps to improve treatment effectiveness and cut down on energy usage.

Reaction Time

Reaction time provides a meaningful impact on the performance of the novel electrochemical precipitation time. Under operational parameters of 0.5cm electrode gap, 5 amps power supply, and same electrode configuration, a significant change in hardness removal was observed in the experiment. While being treated for 15 minutes, the hardness removal rate was 17.3 percent; this rate increased with the reaction time.

At the end of 60 minutes of treatment in all configurations, the hardness removal rate also increased. From Figure 29, it can be observed that 10% graphite concrete cathode showed 20.7% hardness removal in 30 minutes, and it increased to 26% in 60 minutes. Similar results were seen with all other cathodes. It could be observed that with increased time of treatment, the hardness removal efficiency was growing as well. Similar results were found by (Clauwaert et al., 2020; Kalash et al., 2015a; Sanjuán et al., 2019b; Yu et al., 2018a).

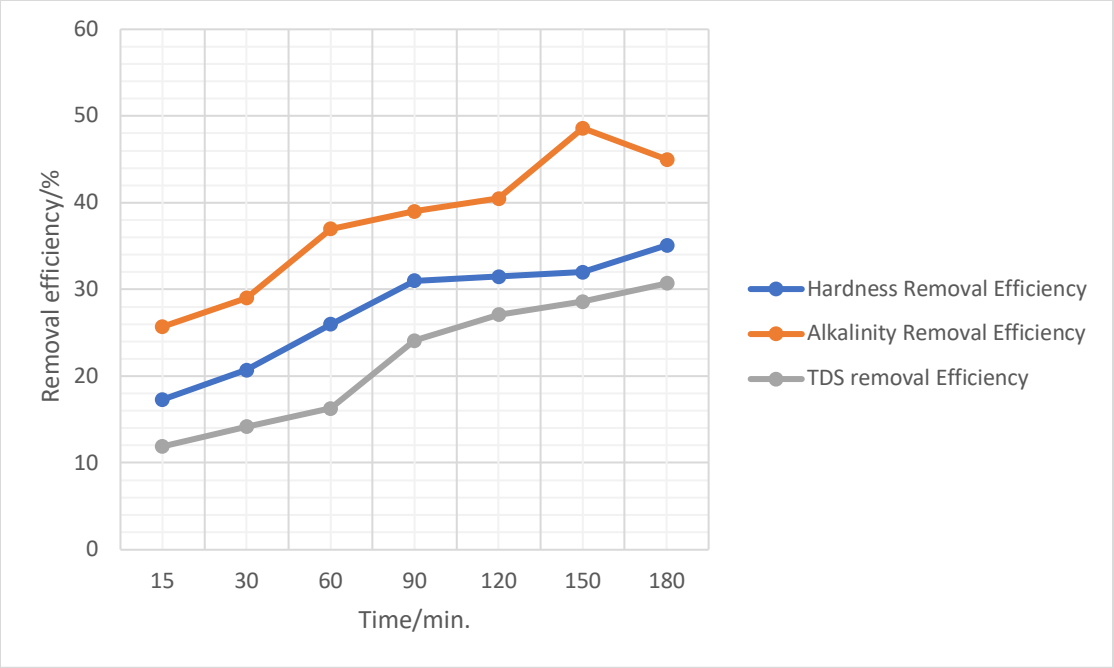

Figure 29: Changes of water quality indexes during 3 hr. continuous operation.

It is reasonable to assume that the cathode's surface is relatively clean in the early stages of the reaction, preventing scale particles from effectively deposition on the cathode and instead flowing out of the reactor with the effluent. As a result, there was a process in which the hardness removal rate and TDS removal rate decreased. After the reaction has been going on for some time, the cathode's surface clearly has scale attached to it. This encourages the growth of scale particles over time, which raises the rate at which hardness and TDS are removed from the water and tends to stabilize with system operation. The cathodic surface scale does not require to be thoroughly cleaned, and appropriate retention of some residual scale can facilitate the rapid and effective electrochemical scale deposition in the next stage.

Ph and Alkalinity

Different effects of pH on the effectiveness of the electrochemical precipitation procedure were seen in earlier research. According to (Malakootian et al., 2010), pH significantly affects how well the electrochemical precipitation works. A higher initial pH is said to improve the effectiveness of hardness reduction. However, it is demonstrated in (Kalash et al., 2015a) that pH had little to no effect on how well an electrochemical precipitation cell removed hardness. However, it was noted in every reference that the pH of the water rises considerably in a successful electrochemical precipitation cell. Similar findings were obtained in this study (Table 9) using a 10% graphite concrete cathode configuration, where the final pH increased from 7.19 to 8.76 after 60 minutes of treatment. No matter the retention duration or the amount of graphite in the cathodes, other test findings revealed comparable outcomes.

Additionally, this study examined the water's decrease in alkalinity. These waters included carbonate alkalinity as CaCO3. Alkalinity significantly decreased when hardness was reduced. But this hardness drop in the alkalinity was far less than actual hardness removed from the water. 10% graphite concrete removed 79.75 mg/L as $CaCO_3$, where alkalinity removal was 26.4 mg/L as $CaCO_3$ for the treatment time of 60 minutes. Similar results were seen in all the retention time and setups.

Table 7: pH and alkalinity change in electrochemical precipitation setup

Electrode	Treatment time	Initial pH	Final pH
10%graphite	60	7.19	8.76
10%graphite	45	7.2	8.23
10%graphite	30	7.2	7.72
10%graphite	15	7.2	7.63

Compressive Strength

To verify the structural integrity of the 10% graphite concrete specimen, its compressive strength was determined. Three cylindrical specimens with a 10 cm diameter and 20 cm length underwent testing. Peak load bearing capability was noted as lateral load was applied. The specimen's detailed results are shown in table (8). The ideal compressive strength for regular concrete is between 2500 and 4000 psi. These specimens' lack of compressive strength can be attributed to one of two factors, the first of which is the aggregate's size. The performance of concrete is greatly influenced by the size of the coarse aggregate. (Tasdemir et al., 1996; Mihashi et al., 1991) Concrete exhibits a heterogeneous behavior and does not fracture linearly. As a result, applying linear fracture mechanics to concrete becomes incredibly challenging. Therefore, the appropriate fracture processes have been identified as fracture energy and fracture toughness.

These aid in describing the concrete's resistance-to-force characteristics. An experiment revealed that adding more coarse aggregate to concrete might increase fracture energy by up to 2.5 times (Chen and Liu, 2004). In this experiment, 9.5mm aggregates were used. In low strength concrete, the size of this aggregate can be crucial. The specimen's high graphite content is the second cause of the low compressive strength. It has been observed that conductive concrete's compressive strength decreases noticeably as graphite content rises.

Table 8: Compressive strength test of 10% graphite concrete cylinder

Specimen	Weight (lb)	Load	Area (Sq. Inch)	Compressive Strength (psi)
10 T1	7.55	11920	12.566	948.59
10 T2	7.55	10855		863.83
10 T3	7.60	9960		792.614

CHAPTER VI

CONCLUSION

To determine the best operating circumstance for the unique electrochemical precipitation system, several experiments were carried out. The tests were carried out in lab-scale continuous procedures. Reaction time, current density and flow rate were found to have an impact on operations. From 2.7% to 35.1%, the hardness removal efficiency was noted. The operational condition of 5 ampere, 30 volts,.5 cm inter-electrode distance, 180 minutes of treatment, and 10% graphite concrete cathode resulted in the maximum hardness elimination. As a result, it was shown that this procedure might be employed as a pretreatment step for removing water hardness. To incorporate conductive concrete into large-scale treatment programs, additional research on the material's structural stability is required. Additionally, it is crucial to conduct more research on the treatment facility's economic viability. Because in electrochemical treatment methods, effective and acceptable energy usage and operational costs are essential to the success of real-world applications. There is a need for more large-scale practical investigations and pilot-scale research.

REFERENCES

Abdualla, H., Ceylan, H., Kim, S., Mina, M., Cetin, K.S., Taylor, P.C., Gopalakrishnan, K., Cetin, B., Yang, S., Vidyadharan, A., 2018. Design and Construction of the World's First Full-Scale Electrically Conductive Concrete Heated Airport Pavement System at a U.S. Airport. Transportation Research Record 2672, 82–94. https://doi.org/10.1177/0361198118791624

Agostinho, L.C.L., Nascimento, L., Cavalcanti, B.F., 2012. Water hardness removal for industrial use: application of the electrolysis process. Open Access Sci Rep 1, 460–465.

Aguilar, M.I., Sáez, J., Lloréns, M., Soler, A., Ortuño, J.F., Meseguer, V., Fuentes, A., 2005. Improvement of coagulation–flocculation process using anionic polyacrylamide as coagulant aid. Chemosphere 58, 47–56. https://doi.org/10.1016/j.chemosphere.2004.09.008

Ahmadzadeh, S., Asadipour, A., Pournamdari, M., Behnam, B., Rahimi, H.R., Dolatabadi, M., 2017. Removal of ciprofloxacin from hospital wastewater using electrocoagulation technique by aluminum electrode: Optimization and modelling through response surface methodology. Process Safety and Environmental Protection 109, 538–547. https://doi.org/10.1016/j.psep.2017.04.026

Anglada, Á., Urtiaga, A., Ortiz, I., 2009. Contributions of electrochemical oxidation to waste-water treatment: fundamentals and review of applications. Journal of Chemical Technology & Biotechnology 84, 1747–1755. https://doi.org/10.1002/jctb.2214

Arabzadeh, A., Sassani, A., Ceylan, H., Kim, S., Gopalakrishnan, K., Taylor, P.C., 2019. Comparison between cement paste and asphalt mastic modified by carbonaceous materials: Electrical and thermal properties. Construction and Building Materials 213, 121–130. https://doi.org/10.1016/j.conbuildmat.2019.04.060

Barrera-Díaz, C., Frontana-Uribe, B., Bilyeu, B., 2014. Removal of organic pollutants in industrial wastewater with an integrated system of copper electrocoagulation and electrogenerated H2O2. Chemosphere 105, 160–164. https://doi.org/10.1016/j.chemosphere.2014.01.026

Becker, H.A., Cohen, J.J., Zdunek, A.D., 2009. Electrochemical cooling water treatment: a new strategy for control of hardness, scale, sludge and reducing water usage. ASHRAE Transactions 115, 399–405.

Bequet, S., Abenoza, T., Aptel, P., Espenan, J.-M., Remigy, J.-C., Ricard, A., 2000. New composite membrane for water softening. Desalination 131, 299–305. https://doi.org/10.1016/S0011-9164(00)90028-6

Bergman, R., 1995. Florida: a cost comparison update: membrane softening vs. lime softening. International Desalination & Water Reuse Quarterly 5, 35–43.

Brastad, K.S., He, Z., 2013. Water softening using microbial desalination cell technology. Desalination 09, 32–37. https://doi.org/10.1016/j.desal.2012.09.01

Cañizares, P., Paz, R., Sáez, C., Rodrigo, M.A., 2009. Costs of the electrochemical oxidation of wastewaters: A comparison with ozonation and Fenton oxidation processes. Journal of Environmental Management 90, 410–420. https://doi.org/10.1016/j.jenvman.2007.10.010

Casqueira, R.G., Torem, M.L., Kohler, H.M., 2006. The removal of zinc from liquid streams by electroflotation. Minerals Engineering 19, 1388–1392. https://doi.org/10.1016/j.mineng.2006.02.001

Ceylan, H., Gopalakrishnan, K., Kim, S., 2014. Heated Transportation Infrastructure Systems: Existing ande Emerging Technologies 16.

Chen, B., Liu, J., 2004. Effect of aggregate on the fracture behavior of high strength concrete. Construction and Building Materials 18, 585–590. https://doi.org/10.1016/j.conbuildmat.2004.04.013

Chen, G., 2004. Electrochemical technologies in wastewater treatment. Separation and purification Technology 38, 11–41.

Clauwaert, P., De Paepe, J., Jiang, F., Alonso-Fariñas, B., Vaiopoulou, E., Verliefde, A., Rabaey, K., 2020. Electrochemical tap water softening: A zero chemical input approach. Water Research 169, 115263. https://doi.org/10.1016/j.watres.2019.115263

Comninellis, C., Chen, G., 2010. Electrochemistry for the Environment. Springer.

da Cruz, S.G., Dutra, A.J., Monte, M.B., 2016. The influence of some parameters on bubble average diameter in an electroflotation cell by laser diffraction method. Journal of environmental chemical engineering 4, 3681–3687.

Emamjomeh, Mohammad.M., Sivakumar, Muttucumaru., 2009. Review of pollutants removed by electrocoagulation and electrocoagulation/flotation processes. Journal of Environmental Management 90, 1663–1679. https://doi.org/10.1016/j.jenvman.2008.12.011

Entezari, M.H., Tahmasbi, M., 2009. Water softening by combination of ultrasound and ion exchange. Ultrasonics Sonochemistry 16, 356–360. https://doi.org/10.1016/j.ultsonch.2008.09.008

Fajardo, A.S., Martins, R.C., Quinta-Ferreira, R.M., 2014. Treatment of a Synthetic Phenolic Mixture by Electrocoagulation Using Al, Cu, Fe, Pb, and Zn as Anode Materials. Ind. Eng. Chem. Res. 53, 18339–18345. https://doi.org/10.1021/ie502575d

Fajardo, A.S., Martins, R.C., Silva, D.R., Martínez-Huitle, C.A., Quinta-Ferreira, R.M., 2017. Dye wastewaters treatment using batch and recirculation flow electrocoagulation systems. Journal of Electroanalytical Chemistry 801, 30–37. https://doi.org/10.1016/j.jelechem.2017.07.015

Fu, L., Wang, J., Su, Y., 2009. Removal of low concentrations of hardness ions from aqueous solutions using electrodeionization process. Separation and Purification Technology 68, 390–396. https://doi.org/10.1016/j.seppur.2009.06.010

Gabrielli, C., Maurin, G., Francy-Chausson, H., Thery, P., Tran, T.T.M., Tlili, M., 2006. Electrochemical water softening: principle and application. Desalination 201, 150–163. https://doi.org/10.1016/j.desal.2006.02.012

Ghizellaoui, S., Taha, S., Dorange, G., Chibani, A., Gabon, J., 2005. Softening of Hamma drinking water by nanofiltration and by lime in the presence of heavy metals. Desalination 171, 133–138. https://doi.org/10.1016/j.desal.2004.05.001

Gönder, Z.B., Balcıoğlu, G., Vergili, I., Kaya, Y., 2017. Electrochemical treatment of carwash wastewater using Fe and Al electrode: Techno-economic analysis and sludge characterization. Journal of Environmental Management 200, 380–390. https://doi.org/10.1016/j.jenvman.2017.06.005

Gude, V.G., 2015. Energy storage for desalination processes powered by renewable energy and waste heat sources. Applied Energy 137, 877–898. https://doi.org/10.1016/j.apenergy.2014.06.061

Hasson, D., Lumelsky, V., Greenberg, G., Pinhas, Y., Semiat, R., 2008. Development of the electrochemical scale removal technique for desalination applications. Desalination 230, 329–342.

Hasson, D., Sidorenko, G., Semiat, R., 2011. Low electrode area electrochemical scale removal system. Desalination and Water Treatment 31, 35–41. https://doi.org/10.5004/dwt.2011.2389

Hasson, D., Sidorenko, G., Semiat, R., 2010. Calcium carbonate hardness removal by a novel electrochemical seeds system. Desalination 263, 285–289. https://doi.org/10.1016/j.desal.2010.06.036

Hayashi, M., 2004. Temperature-Electrical Conductivity Relation of Water for Environmental Monitoring and Geophysical Data Inversion. Environ Monit Assess 96, 119–128. https://doi.org/10.1023/B:EMAS.0000031719.83065.68

Hernández, I.L., Díaz, C.B., Cerecero, M.V., Sánchez, P.T.A., Juárez, M.C., Lugo, V.L., 2017. Soft drink wastewater treatment by electrocoagulation–electrooxidation processes. Environmental Technology 38, 433–442. https://doi.org/10.1080/09593330.2016.1196740

Hosny, A.Y., 1996. Separating oil from oil-water emulsions by electroflotation technique. Separations Technology 6, 9–17. https://doi.org/10.1016/0956-9618(95)00136-0

Janssen, L.J.J., Sillen, C.W.M.P., Barendrecht, E., van Stralen, S.J.D., 1984. Bubble behaviour during oxygen and hydrogen evolution at transparent electrodes in KOH solution. Electrochimica Acta 29, 633–642. https://doi.org/10.1016/0013-4686(84)87122-4

Jin, H., Yu, Y., Zhang, L., Yan, R., Chen, X., 2019. Polarity reversal electrochemical process for water softening. Separation and Purification Technology 210, 943–949. https://doi.org/10.1016/j.seppur.2018.09.009

Jury, W.A., Vaux, H., 2005. The role of science in solving the world's emerging water problems. Proceedings of the National Academy of Sciences 102, 15715–15720. https://doi.org/10.1073/pnas.0506467102

Kabay, N., Demircioglu, M., Ersöz, E., Kurucaovali, I., 2002. Removal of calcium and magnesium hardness by electrodialysis. Desalination 149, 343–349. https://doi.org/10.1016/S0011-9164(02)00807-X

Kalash, K.R., Ghazi, I.N., Abdul-Majeed, M.A., 2015a. Hardness Removal from Drinking Water Using Electrochemical Cell 12.

Kalash, K.R., N.Ghazi, I., Abdul-Majeed, M.A., 2015b. Hardness Removal from Drinking Water Using Electrochemical Cell. Engineering and Technology Journal 33, 78–89.

Kenny, J.F., Barber, N.L., Hutson, S.S., Linsey, K.S., Lovelace, J.K., Maupin, M.A., 2009. Estimated use of water in the United States in 2005 (USGS Numbered Series No. 1344), Estimated use of water in the United States in 2005, Circular. U.S. Geological Survey, Reston, VA. https://doi.org/10.3133/cir1344

Lédion, J., Leroy, P., 1994. Nouvelle méthode d'évaluation des procédés «antitartre» physiques. La Tribune de l'eau 47, 43–49.

Lee, J.-B., Park, K.-K., Eum, H.-M., Lee, C.-W., 2006. Desalination of a thermal power plant wastewater by membrane capacitive deionization. Desalination 196, 125–134. https://doi.org/10.1016/j.desal.2006.01.011

Legrand, L., Poirier, G., Leroy, P., 1981. Les équilibres carboniques et léquilibre calcocarbonique dans les eaux naturelles: étude graphique, utilisation de calculatrices. Eyrolles.

Li, X., Wang, L., Sun, W., Yan, Z., He, Y., Shu, X., Liu, G., 2020. Study on electrochemical water softening mechanism of high-efficient multi-layer mesh coupled cathode. Separation and Purification Technology 247, 117001. https://doi.org/10.1016/j.seppur.2020.117001

Lima, R.A.C., Santos, S.R.B., Costa, R.S., Marcone, G.P.S., Honorato, R.S., Nascimento, V.B., Araujo, M.C.U., 2004. Hardness screening of water using a flow-batch photometric system. Analytica Chimica Acta 518, 25–30. https://doi.org/10.1016/j.aca.2004.05.013

Liu, A., Liu, S., 2016. Study on performance of three backwashing modes of filtration media for oilfield wastewater filter. Desalination and Water Treatment 57, 10498–10505.

Low, S.C., Liping, C., Hee, L.S., 2008. Water softening using a generic low cost nano-filtration membrane. Desalination 221, 168–173. https://doi.org/10.1016/j.desal.2007.04.064

Luan, J., Wang, L., Sun, W., Li, X., Zhu, T., Zhou, Y., Deng, H., Chen, S., He, S., Liu, G., 2019. Multi-meshes coupled cathodes enhanced performance of electrochemical water softening system. Separation and Purification Technology 217, 128–136. https://doi.org/10.1016/j.seppur.2019.01.054

Maksimov, E.A., Ostsemin, A.A., 2015. Intensifying the cleaning of emulsion-and oil-bearing waste water from rolled-product manufacturing by electroflotation. Metallurgist 58, 945–949.

Malakootian, M., Mansoorian, H.J., Moosazadeh, M., 2010. Performance evaluation of electrocoagulation process using iron-rod electrodes for removing hardness from drinking water. Desalination 255, 67–71. https://doi.org/10.1016/j.desal.2010.01.015

Martínez-Huitle, C.A., Ferro, S., 2006. Electrochemical oxidation of organic pollutants for the wastewater treatment: direct and indirect processes. Chem. Soc. Rev. 35, 1324–1340. https://doi.org/10.1039/B517632H

Martínez-Huitle, C.A., Rodrigo, M.A., Scialdone, O., 2018. Electrochemical Water and Wastewater Treatment. Butterworth-Heinemann.

Martínez-Huitle, C.A., Rodrigo, M.A., Sirés, I., Scialdone, O., 2015. Single and Coupled Electrochemical Processes and Reactors for the Abatement of Organic Water Pollutants: A Critical Review. Chem. Rev. 115, 13362–13407. https://doi.org/10.1021/acs.chemrev.5b00361

Mihashi, H., Nomura, N., Niiseki, S., 1991. Influence of aggregate size on fracture process zone of concrete detected with three dimensional acoustic emission technique. Cement and Concrete Research 21, 737–744. https://doi.org/10.1016/0008-8846(91)90168-H

Moran, S., 2018. Chapter 8 - Clean water unit operation design: Chemical processes, in: Moran, S. (Ed.), An Applied Guide to Water and Effluent Treatment Plant Design. Butterworth-Heinemann, pp. 101–110. https://doi.org/10.1016/B978-0-12-811309-7.00008-4

Notani, M.A., Arabzadeh, A., Ceylan, H., Kim, S., Gopalakrishnan, K., 2019. Effect of Carbon-Fiber Properties on Volumetrics and Ohmic Heating of Electrically Conductive Asphalt Concrete. J. Mater. Civ. Eng. 31, 04019200. https://doi.org/10.1061/(ASCE)MT.1943-5533.0002868

Organization, W.H., 2010. Hardness in drinking-water: background document for development of WHO guidelines for drinking-water quality. World Health Organization.

Pan, P., Wu, S., Xiao, Y., Liu, G., 2015. A review on hydronic asphalt pavement for energy harvesting and snow melting. Renewable and Sustainable Energy Reviews 48, 624–634. https://doi.org/10.1016/j.rser.2015.04.029

Park, J.-S., Song, J.-H., Yeon, K.-H., Moon, S.-H., 2007. Removal of hardness ions from tap water using electromembrane processes. Desalination 202, 1–8. https://doi.org/10.1016/j.desal.2005.12.031

Park, N.S., Yoon, S.M., Kim, S.H., Kim, J.O., 2016. Effects of bubble size on air-scoured backwashing efficiency in a biofilter. Desalination and Water Treatment 57, 7538–7544. https://doi.org/10.1080/19443994.2015.1024936

Perez, L.A., Freese, D.T., 1997. Scale Prevention at High Lsi, High Cycles, And High Ph Without The Need For Acid Feed. Presented at the Corrosion97, OnePetro.

Rajeshwar, K., Ibanez, J.G., 1997. Environmental Electrochemistry: Fundamentals and Applications in Pollution Sensors and Abatement. Elsevier.

Sadati, S.M.S., Cetin, K., Ceylan, H., Sassani, A., Kim, S., 2018. Energy and thermal performance evaluation of an automated snow and ice removal system at airports using numerical modeling and field measurements. Sustainable Cities and Society 43, 238–250. https://doi.org/10.1016/j.scs.2018.08.021

Sahu, O., Rao, D.G., Gopal, R., Tiwari, A., Pal, D., 2017. Treatment of wastewater from sugarcane process industry by electrochemical and chemical process: Aluminum (metal and salt). Journal of Water Process Engineering 17, 50–62. https://doi.org/10.1016/j.jwpe.2017.03.005

Sanjuán, I., Benavente, D., Expósito, E., Montiel, V., 2019a. Electrochemical water softening: Influence of water composition on the precipitation behaviour. Separation and Purification Technology 211, 857–865. https://doi.org/10.1016/j.seppur.2018.10.044

Sanjuán, I., García-García, V., Expósito, E., Montiel, V., 2019b. Paired electrolysis for simultaneous electrochemical water softening and production of weak acid solutions.

Electrochemistry Communications 101, 88–92. https://doi.org/10.1016/j.elecom.2019.03.002

Sarkar, M.S.K.A., Donne, S.W., Evans, G.M., 2011. Utilization of hydrogen in electroflotation of silica. Advanced Powder Technology, Special Issue Featuring Articles from Chemeca2010 22, 482–492. https://doi.org/10.1016/j.apt.2011.05.007

Sassani, A., Ceylan, H., Kim, S., Arabzadeh, A., Taylor, P.C., Gopalakrishnan, K., 2018. Development of Carbon Fiber-modified Electrically Conductive Concrete for Implementation in Des Moines International Airport. Case Studies in Construction Materials 8, 277–291. https://doi.org/10.1016/j.cscm.2018.02.003

Sassani, A., Ceylan, H., Kim, S., Gopalakrishnan, K., Arabzadeh, A., Taylor, P.C., 2017. Influence of mix design variables on engineering properties of carbon fiber-modified electrically conductive concrete. Construction and Building Materials 152, 168–181. https://doi.org/10.1016/j.conbuildmat.2017.06.172

Saurina, J., López-Aviles, E., Le Moal, A., Hernández-Cassou, S., 2002. Determination of calcium and total hardness in natural waters using a potentiometric sensor array. Analytica Chimica Acta 464, 89–98. https://doi.org/10.1016/S0003-2670(02)00474-9

Sengupta, P., 2013. Potential Health Impacts of Hard Water. Int J Prev Med 4, 866–875.

Sirés, I., Brillas, E., Oturan, M.A., Rodrigo, M.A., Panizza, M., 2014. Electrochemical advanced oxidation processes: today and tomorrow. A review. Environ Sci Pollut Res 21, 8336–8367. https://doi.org/10.1007/s11356-014-2783-1

Soltanieh, M., Mousavi, M., 1999. Application of charged membranes in water softening: modeling and experiments in the presence of polyelectrolytes. Journal of Membrane Science 154, 53–60. https://doi.org/10.1016/S0376-7388(98)00285-3

Song, F., Zhang, N., Smith, R., Zeng, Y., Li, J., Xiao, X., 2018. Simultaneous Optimization for Integrated Cooling Water System with Chemical Processes, in: Friedl, A., Klemeš, J.J., Radl, S., Varbanov, P.S., Wallek, T. (Eds.), Computer Aided Chemical Engineering, 28 European Symposium on Computer Aided Process Engineering. Elsevier, pp. 477–482. https://doi.org/10.1016/B978-0-444-64235-6.50085-1

Subba Rao, A.N., Venkatarangaiah, V.T., 2014. Metal oxide-coated anodes in wastewater treatment. Environ Sci Pollut Res 21, 3197–3217. https://doi.org/10.1007/s11356-013-2313-6

Sun, J., Lin, S., Zhang, G., Sun, Y., Zhang, J., Chen, C., Morsy, A.M., Wang, X., 2021. The effect of graphite and slag on electrical and mechanical properties of electrically conductive cementitious composites. Construction and Building Materials 281, 122606. https://doi.org/10.1016/j.conbuildmat.2021.122606

Tabatabai, A., Scamehorn, J.F., Christian, S.D., 1995. Economic feasibility study of polyelectrolyte-enhanced ultrafiltration (PEUF) for water softening. Journal of Membrane Science 100, 193–207. https://doi.org/10.1016/0376-7388(94)00220-S

Tasdemir, C., Tasdemir, M.A., Lydon, F.D., Barr, B.I.G., 1996. Effects of silica fume and aggregate size on the brittleness of concrete. Cement and Concrete Research 26, 63–68. https://doi.org/10.1016/0008-8846(95)00180-8

Tlili, M.M., Amor, M.B., Gabrielli, C., Joiret, S., Maurin, G., Rousseau, P., 2003a. Study of electrochemical deposition of CaCO3 by in situ raman spectroscopy: II. Influence of the solution composition. Journal of The Electrochemical Society 150, C485.

Tlili, M.M., Benamor, M., Gabrielli, C., Perrot, H., Tribollet, B., 2003b. Influence of the interfacial pH on electrochemical CaCO3 precipitation. Journal of the Electrochemical Society 150, C765.

Valero, F., Arbós, R., 2010. Desalination of brackish river water using Electrodialysis Reversal (EDR): Control of the THMs formation in the Barcelona (NE Spain) area. Desalination 253, 170–174. https://doi.org/10.1016/j.desal.2009.11.011

Vasudevan, S., Lakshmi, J., Sozhan, G., 2013. Electrochemically assisted coagulation for the removal of boron from water using zinc anode. Desalination, Removal of Boron from Seawater, Geothermal Water and Wastewater 310, 122–129. https://doi.org/10.1016/j.desal.2012.01.016

Vasudevan, S., Lakshmi, J., Sozhan, G., 2011. Studies on the Al–Zn–In-alloy as anode material for the removal of chromium from drinking water in electrocoagulation process. Desalination 275, 260–268. https://doi.org/10.1016/j.desal.2011.03.011

Vasudevan, S., Lakshmi, J., Sozhan, G., 2009. Studies on a Mg-Al-Zn Alloy as an Anode for the Removal of Fluoride from Drinking Water in an Electrocoagulation Process. CLEAN – Soil, Air, Water 37, 372–378. https://doi.org/10.1002/clen.200900031

Viero, A.F., Mazzarollo, A.C.R., Wada, K., Tessaro, I.C., 2002. Removal of hardness and COD from retanning treated effluent by membrane process. Desalination 149, 145–149. https://doi.org/10.1016/S0011-9164(02)00746-4

Wang, D., Tang, H., Gregory, J., 2002. Relative importance of charge neutralization and precipitation on coagulation of kaolin with PACl: effect of sulfate ion. Environmental science & technology 36, 1815–1820.

Wang, J., Shi, M., Zhang, G., 2018. Effects of Operational Conditions on Electrochemical Water Softening Using DSA Anode, in: Proceedings of the 2018 7th International Conference on Energy and Environmental Protection (ICEEP 2018). Presented at the 2018 7th International Conference on Energy and Environmental Protection (ICEEP 2018), Atlantis Press, Shenzhen, China. https://doi.org/10.2991/iceep-18.2018.215

Wu, W., Huang, Z.-H., Lim, T.-T., 2014. Recent development of mixed metal oxide anodes for electrochemical oxidation of organic pollutants in water. Applied Catalysis A: General 480, 58–78. https://doi.org/10.1016/j.apcata.2014.04.035

Yeon, K.-H., Song, J.-H., Moon, S.-H., 2004. A study on stack configuration of continuous electrodeionization for removal of heavy metal ions from the primary coolant of a nuclear power plant. Water Research 38, 1911–1921. https://doi.org/10.1016/j.watres.2004.01.003

Yeon, K.-H., Song, J.-H., Shim, J., Moon, S.-H., Jeong, Y.-U., Joo, H.-Y., 2007. Integrating electrochemical processes with electrodialysis reversal and electro-oxidation to minimize COD and T-N at wastewater treatment facilities of power plants. Desalination, Wastewater Reclamation and Reuse for Sustainability 202, 400–410. https://doi.org/10.1016/j.desal.2005.12.080

Yildiz, E., Nuhoglu, A., Keskinler, B., Akay, G., Farizoglu, B., 2003. Water softening in a crossflow membrane reactor. Desalination 159, 139–152. https://doi.org/10.1016/S0011-9164(03)90066-X

Yu, Y., Jin, H., Jin, X., Yan, R., Zhang, L., Chen, X., 2018a. Current Pulsated Electrochemical Precipitation for Water Softening. Ind. Eng. Chem. Res. 57, 6585–6593. https://doi.org/10.1021/acs.iecr.8b00448

Yu, Y., Jin, H., Meng, P., Guan, Y., Shao, S., Chen, X., 2018b. Electrochemical water softening using air-scoured washing for scale detachment. Separation and Purification Technology 191, 216–224. https://doi.org/10.1016/j.seppur.2017.09.032

Yu, Y., Jin, H., Meng, P., Guan, Y., Shao, S., Chen, X., 2018c. Electrochemical water softening using air-scoured washing for scale detachment. Separation and Purification Technology 191, 216–224. https://doi.org/10.1016/j.seppur.2017.09.032

Yu, Y., Jin, H., Quan, X., Hong, B., Chen, X., 2019. Continuous Multistage Electrochemical Precipitation Reactor for Water Softening. Ind. Eng. Chem. Res. 58, 461–468. https://doi.org/10.1021/acs.iecr.8b04200

Zeng, Y., Yang, C., Pu, W., Zhang, X., 2007. Removal of silica from heavy oil wastewater to be reused in a boiler by combining magnesium and zinc compounds with coagulation. Desalination 216, 147–159. https://doi.org/10.1016/j.desal.2007.01.005

Zhi, S., Zhang, K., 2016. Hardness removal by a novel electrochemical method. Desalination 381, 8–14. https://doi.org/10.1016/j.desal.2015.12.002

Appendix

APPENDIX

Experimental Data

Table 19: Summary of total experimental data

Initial Hardness (mg/L)	Initial Alkalinity (mg/L)	Initial TDS (mg/L)	Reaction Time (mins.)	Final Hardness (mg/L)	Final Alkalinity (mg/L)	Final TDS (mg/L)
290	74	710	15	239.8	55	625.5
290	74	710	30	230	59.2	609.2
290	74	710	60	214.6	46.6	594.3
290	74	710	90	200.1	44.4	538.9
290	74	710	120	198.7	47.3	517.6
290	74	710	150	197.2	38	506.94
290	74	710	180	188.21	40.7	492

BIOGRAPHICAL SKETCH

Tahsin Tareque was born in Bangladesh. He completed his B.Sc. in Civil Engineering from Islamic University of Technology. He studied MS in civil Engineering at University of Texas Rio Grande Valley (UTRGV). He completed Master of Science in Civil Engineering from University of Texas Rio Grande Valley (UTRGV) in December 2022. His email address is Tahsintareque@gmail.com. His permanent address was Sylhet, Bangladesh. He likes to play cricket, football, and Tennis.